Published in final edited form as:

J Cell Physiol. 2009 August ; 220(2): 382–393. doi:10.1002/jcp.21777.

Activation of Src Kinase by Protein–Tyrosine Phosphatase–PEST in Osteoclasts: Comparative Analysis of the Effects of Bisphosphonate and Protein–Tyrosine Phosphatase Inhibitor on Src Activation In Vitro

MEENAKSHI A. CHELLAIAH[1,*], **MICHAEL D. SCHALLER**[2]

[1]Department of Oncology and Diagnostic Sciences, Dental School, University of Maryland, Baltimore, Maryland [2]Department of Biochemistry, West Virginia University, Morgantown, West Virginia

Abstract

PTP–PEST is involved in the regulation of sealing ring formation in osteoclasts. In this article, we have shown a regulatory role for PTP–PEST on dephosphorylation of c-Src at Y527 and phosphorylation at Y418 in the catalytic site. Activation of Src in osteoclasts by over-expression of PTP–PEST resulted in the phosphorylation of cortactin at Y421 and WASP at Y294. Also enhanced as a result, is the interaction of Src, cortactin, and Arp2 with WASP. Moreover, the number of osteoclasts displaying sealing ring and bone resorbing activity was increased in response to PTP–PEST over-expression as compared with control osteoclasts. Cells expressing constitutively active-Src (527YDF) simulate the effects mediated by PTP–PEST. Treatment of osteoclasts with a bisphosphonate alendronate or a potent PTP inhibitor PAO decreased the activity and phosphorylation of Src at Y418 due to reduced dephosphorylation state at Y527. Therefore, Src-mediated phosphorylation of cortactin and WASP as well as the formation of WASP cortactin Arp2 complex and sealing ring were reduced in these osteoclasts. Similar effects were observed in osteoclasts treated with [C1]an Src inhibitor PP2. We have shown that bisphosphonates could modulate the function of osteoclasts by inhibiting downstream signaling mediated by PTP–PEST/Src, in addition to its effect on the inhibition of the post-translational modification of small GTP-binding proteins such as Rab, Rho, and Rac as shown by others. The promising effects of the inhibitors PP2 and PAO on osteoclast function suggest a therapeutic approach for patients with bone metastases and osteoporosis as an alternative to bisphosphonates.

Sealing ring formation is a requirement in osteoclast bone resorption. Distinct pathways and molecules including Src, PYK2, c-Cbl, p130Cas, PTP–PEST, RhoGTPases, PI3-kinase, and WASP have been known to play roles in the organization of the sealing ring during bone resorption (Murakami et al., 1995; Zhang et al., 1995; Duong et al., 1998; Chellaiah et al., 2001; Gupta et al., 2003; Chellaiah, 2006; Sanjay et al., 2006). WASP-deficient cells are markedly depleted of podosomes and fail to exhibit sealing rings. Complementation of

[*]Correspondence to: Meenakshi A. Chellaiah, Department of Oncology and Diagnostic Sciences, Dental School, University of Maryland, Baltimore, MD. mchellaiah@umaryland.edu.

WASP-null osteoclasts with an enhanced GFP-WASP fusion protein restores normal cytoarchitecture (Calle et al., 2004). We have previously demonstrated that WASP integrates signals from Rho, Cdc42, and kinase(s) in order to bind to the Arp2/3 complex and stimulate Arp2/3-dependent actin polymerization and sealing ring formation (Chellaiah, 2005; Chellaiah et al., 2007).

WASP is a binding partner for c-Src SH3 domain (Banin et al., 1996a; Schulte and Sefton, 2003). Phosphorylation of WASP at Y291 increases the stability of activated WASP and blocks the inhibitory interaction between GBD and the VCA domain (Cory et al., 2003). In osteoclasts, Src regulates the phosphorylation of WASP at Y291, which is critical for osteoclast bone resorption. Phosphorylated WASP at Y291 interacts with c-Src, PYK2, PTP–PEST, PST-PIP, cortactin, and p160 kDa proteins (identified as Rho kinase). Phosphorylation of these proteins and WASP was markedly increased in osteoclasts that express constitutively active-Src (CA-Src) (Chellaiah et al., 2007). Osteoclasts transduced with TAT- fused WASP peptide containing pTyr294 (pTyr291 in humans and pTyr294 in mice) demonstrated a decrease in the interaction of Src with endogenous WASP, loss of sealing ring formation, and reduced capacity for bone resorption. Modulation of tyrosine phosphorylation state of pTyr291 in WASP assists in integrating multiple signaling molecules and pathway(s) that assist in the assembly of sealing ring (Ma et al., 2008).

Several tyrosine phosphatases (PTP, PTPRO, PTP-epsilon, SHP-1, and PTP–PEST) are present in osteoclasts and they appear to assist in osteoclast function (reviewed in Gil-Henn and Elson, 2003; Chiusaroli et al., 2004; Chellaiah, 2006; Granot-Attas and Elson, 2008). PTP-epsilon (PTP-ε) knockout mice (EKO mice) exhibit increased trabecular bone due to the reduced function of osteoclasts. The fine structure of podosomes in the osteoclasts of EKO mice is defective due to disorganization of their actin core (Chiusaroli et al., 2004). PTP–PEST contains the typical tyrosine phosphatase catalytic domain flanked by proline-rich regions. These regions are capable of interacting with several signaling molecules, including leupaxin, paxillin, WASP, PYK2, Src, p130Cas, and Grb2 (Garton and Tonks, 1994, 1999; Cote et al., 1998; Gupta et al., 2003; Badour et al., 2004; Chellaiah et al., 2007). We have demonstrated that PTP–PEST regulates podosome assembly/disassembly and sealing formation in mouse osteoclasts (Chellaiah et al., 2001, 2007; Gupta et al., 2003). Our recent studies using the SiRNA to PTP–PEST or an inhibitor to phosphatase (PAO) showed inhibition of osteoclast bone resorption due to derangement of actin cytoskeleton (Chellaiah et al., 2007).

Numerous studies have resulted in significant progress in our understanding of the effects of bisphosphonates (BPs) on osteoclast function. Some of these studies have shown that BPs inhibit a key enzyme called farnesyl pyrophosphate synthase in the mevalonate pathway. Hence, the inhibition of post-translational modification of small GTP-binding proteins such as, Rab, Rho, and Rac by BPs decrease the activity of osteoclasts (Rogers et al., 2000; Dunford et al., 2001; Virtanen et al., 2002; Rogers, 2003; Valleala et al., 2003). Previous studies have also shown that alendronate can reduce the activity of PTPs such as PTP-δ and -ε which correlated with the inhibition of osteoclast bone resorption in vitro (Endo et al., 1996; Schmidt et al., 1996; Opas et al., 1997).

Tyrosine phosphatase PTP1B and PTP-ε were shown to have a role in the activation of Src in colon cancer cells and osteoclasts, respectively (Gil-Henn and Elson, 2003; Zhu et al., 2007). PTP1B activates Src through dephosphorylation of Src at Y530. Elevated levels of PTP1B can increase tumorigenecity of colon cells by activating Src (Zhu et al., 2007). PTP1D is another class of phosphatase (PTP1D and PTP1D2) expressed in a variety of tissues. PTP1D was found to be associated with Src kinase (Moller et al., 1994). Although PTPs such as PTP-δ and -ε are involved in signaling related to osteoclast bone resorption (Endo et al., 1996; Schmidt et al., 1996; Opas et al., 1997), the nature of the molecular targets for these PTPs has yet to be clarified. Recently, we have shown that both tyrosine kinase(s) and the tyrosine phosphatase PTP–PEST coordinate the formation of the sealing ring and thus the bone-resorbing function of osteoclasts. WASP, which is identified in the sealing ring of resorbing osteoclasts, also demonstrates an interaction with c-Src, PYK2, PSTPIP, and PTP–PEST proteins (Chellaiah et al., 2007). The underlying molecular mechanisms involved in the formation of WASP-associated signaling complex formation and the role of PTP–PEST in this process are still poorly understood.

In an attempt to explore the role of PTP–PEST in the formation of sealing ring, we have used osteoclasts null for PTP–PEST or over-expressing PTP–PEST. Since osteoclast bone resorption involves Src as a primary kinase (Boyce et al., 1992) and PTPs regulate the activation of Src (Zhu et al., 2007), we have used osteoclasts expressing CA-Src and kinase-defective-Src (KD-Src) as controls. In the present study we demonstrate that PTP–PEST regulates the activity of Src through dephosphorylation of Src at Y527 (corresponding to Y530 in human). PTPs were shown as a molecular target for BP alendronate (Zhu et al., 2007). We further show that the attenuation of PTP–PEST activity by PAO and alendronate is associated with the decrease in the activity and phosphorylation of Src at Y418. Therefore, Src-mediated phosphorylation of cortactin and WASP as well as the formation of WASP cortactin Arp2 complex and sealing ring were reduced in these osteoclasts.These studies demonstrate that alendronate inhibits downstream signaling mediated by PTP–PEST/Src.

Materials and Methods

Reagents

Protein estimation reagent, molecular weight standards for proteins, and PAGE-reagents were bought from Bio-Rad (Hercules, CA). Antibodies to WASP, Arp-2, c-Src, and pTyrosine were obtained from Santa Cruz, CA. Antibody to Src and anti-phosphotyrosine mAb 4G10 were purchased from Upstate Biotechnology (Lake Placid, NY). The Src inhibitor PP2 (4-amino-5-(4-chloro-phenyl)-7-(*t*-butyl) pyrazolo [3,4-d] pyrimidine) was bought from Calbiochem (La Jolla, CA). Antibodies against phospho-Src Y416 and Y527 were obtained from Cell Signaling (Beverly, MA). Anti-GAPDH antibody was purchased from Abcam, Inc. (Cambridge, MA). Streptavidin-HRP and ECL-reagent were bought from Pierce (Rockford, IL). Polyvinyldifluoride (PVDF) membrane was obtained from Millipore Corp. (Bedford, MA). Rhodamine phalloidin, phenyl arsine oxide (PAO), a rabbit polyclonal antibody against phosphocortactin Y421, and all the other chemicals were purchased from Sigma–Aldrich Chemical Co. (St. Louis, MO).

Preparation of osteoclast precursors from mice

C57/BL6 mice were used for osteoclast preparation as described previously (Chellaiah et al., 2007). These mice were either purchased from Harlan Laboratory (Indianapolis, IN) or generated in the animal house of Dental School, University of Maryland. Breeding and maintenance were carried out as per the guidelines and approval of IACUC. Osteoclasts were generated in vitro using mouse bone marrow cells. Cells isolated from five mice were cultured into 100 mm dishes with 20 ml α-MEM medium supplemented with 10% fetal bovine serum (α−10). After culturing for 24 h, non-adhered cells were layered on histopaque-1077 (Sigma–Aldrich Chemical Co.) and centrifuged at 350g for 15 min at room temperature (RT). The cell layer between the histopaque and the medium was removed and washed with α−10 medium at 2000 rpm for 7 min at RT. Cells were resuspended in α−10 medium and cultured with the appropriate concentrations of mCSF-1 (10 ng/ml) and RANK-L (55–75 ng/ml). After 3 days in culture, medium was replaced with fresh cytokines. Multinucleated osteoclasts were seen from day 4 onwards. To remove the osteoclasts for in vitro bone resorption assay, cells were washed with cold PBS and kept in cell stripper solution (Cellgro, Media Tech, Inc., Hemdon, VA) for 15–30 min. Cell stripper is a non-enzymatic cell dissociation solution designed to gently dislodge adherent cells in tissue culture. After incubation with this solution, cells were removed from the plates by gentle scraping. Some of the removed cells were replated and stained with trypan blue and for tartrate-resistant acid phosphatase (TRAP), an osteoclast marker. Cells excluded trypan blue, and they were 99% TRAP-positive. These TRAP-positive cells were used for bone resorption assay as described previously (Chellaiah et al., 2003) and below.

Transfection of small interfering RNA (SiRNA) for PTP–PEST

SiRNA and scrambled control siRNA sequences for PTP–PEST were purchased from Ambion, Inc., (Austin, TX). Osteoclasts were transfected with SiRNA using streptolysin O permeablization as described previously (Chellaiah et al., 1998). Briefly, osteoclasts were washed twice with permeablization buffer (120 mM KCl, 30 mM NaCl, 10 mM Hepes, pH 7.2, 10 mM EGTA, 10 mM $MgCl_2$; Duncan et al., 1996). Freshly prepared dithiothreitol (5 mM), ATP (1 mM), and 0.5 unit/ml streptolysin O (Sigma, St. Louis, MO) and RNAi sequences at the indicated concentrations were added to the buffer at the time of permeablization. Resealing was achieved by the addition of α−10 medium. Control cells were permeablized as above but in the absence of RNAi sequences. After incubation of osteoclasts for 36–48 h at 37°C, lysates were made and subjected to immunoblotting with an antibody to PTP–PEST to detect the endogenous levels.

Preparation of osteoclast lysate after various treatments

CA- and KD-Src that were generated essentially based on pAdEasy-1 system (He et al., 1998) were used for infection. Virus was propagated as described previously (Willey et al., 2003). PTP–PEST adenoviral construct was generated essentially as described (Playford et al., 2006). Adenovirus containing Src or PTP–PEST was added to osteoclasts at the 10–30 multiplicity of infection in the serum-free medium. Two hours after infection, the medium was replaced with α−10 medium. Expression of Src and PTP–PEST was evaluated by

immunoblotting of the osteoclast lysate with respective antibody after 48–72 h post-infection. Osteoclasts treated with PBS were used as controls.

Some cultures were treated with a protein–tyrosine phosphatase (PTP) inhibitor PAO (100 nM), Src inhibitor PP2 (4-amino-5-(4-chloro-phenyl)-7-(*t*-butyl) pyrazolo [3,4-d] pyrimidine; 100 nM), and BPs (alendronate or pamidronate, 50 μM) at 37°C. BP stocks (1 mM) were made in PBS or sterile H_2O. Stock solution of PP2 was prepared in 100% DMSO (Sigma) and stored at −70°C. Dose-dependent effects of PP2 on Src inhibition was determined by Western analysis with an SrcY418 antibody in the presence of increasing concentrations of PP2 (1, 10, 50, 75, 100, 150, or 200 nM). An increase in the inhibition was observed from 50 nM; maximum effect was found at 75 nM concentration and the inhibitory effect stabilized from 100 to 200 nM. The PP2 concentration (100 nM) used in these experiments was selected on the basis of this study. Cell viability was determined using an in vitro viability assay kit (Sigma) following the manufacturer's instructions.

Following various treatments, osteoclasts were washed three times with cold PBS and lysed in a RIPA buffer (10 mM Tris–HCl, pH 7.2, 150 mM NaCl, 1% deoxycholate, 1% Triton X-100, 0.1% SDS, 1% aprotinin, 2 mM phenylmethylsulfonyl fluoride (PMSF), 100 μM Na_3VO_4, and 1% aprotinin). Cells were rocked on ice for 15 min and scraped off with a cell scraper. Cell lysates were centrifuged at 15,000 rpm for 15 min at 4°C, and the supernatant was saved. Protein contents were measured using the Bio-Rad protein assay reagent.

Purification of GST-fused WASP-GP domain

GTPase binding domain of WASP was generated by cloning PCR-generated inserts into the *EcoR1* and *BamH1* sites of pGEX-2T vector (Linder et al., 1999). pGEX vector and pGEX containing WASP-GP construct were expressed in Escherichia coli as glutathione S-transferase (GST) fusions as described previously (Chellaiah et al., 2001). SDS–PAGE and Coomassie Blue staining tested the purity of the purified proteins.

Immunoprecipitation, GST pulldown, and Western analysis

About 500 μg of protein was used for GST pulldown or immunoprecipitation with a WASP antibody. For immunoprecipitation, lysate proteins were precleared with protein A-Sepharose presoaked in lysis buffer containing bovine serum albumin (BSA) and with non-immune IgG coupled to protein A-Sepharose beads. The precleared supernatants were incubated with antibodies of interest, and the immune complexes were adsorbed onto protein A-Sepharose beads. The beads were pelleted and washed three times for 5 min each with ice-cold PBS and the immune complexes were dissociated by boiling in SDS sample buffer. Pulldown with GST-fused WASP-GP protein or vector protein (GST alone) coupled to Glutathione Sepharose 4B was performed as described previously (Chellaiah et al., 2007). Proteins bound to Glutathione Sepharose 4B beads were then dissociated by boiling in SDS sample buffer after washing three times with cold PBS. The samples were analyzed by SDS–PAGE and Western blotting.

For Western blotting, proteins were transferred to a polyvinylidene difluoride (PVDF) membrane. Blots were blocked with 10% milk in PBS containing 0.5% Tween (PBS-T) for 2–3 h and then incubated with 1:1,000 dilutions of primary antibody of interest for 2–3 h.

After three washes for 10 min each with PBS-T, the blot was incubated with a 1:1,000 dilutions of peroxidaseconjugated species-specific secondary antibody for 2 h at RT. After three washes for 10 min each with PBS-T, protein bands were visualized by chemiluminescence using the ECL kit (Pierce). For immunoblotting analysis with the phosphotyrosine (4G10) antibody, blots were blocked with 5% BSA in PBS-T (Chellaiah et al., 2003).

Immunocytochemistry

Osteoclast precursors (10^5 cell/coverslips) were seeded on dentine slices and incubated for 48–72 h. Osteoclasts were fixed with 3% paraformaldehyde for 20 min and permeablized with 0.1% Triton X-100 in PBS for 5 min as described previously (Chellaiah, 2005). Background fluorescence was blocked with a blocking solution (PBS with 0.2% BSA, 0.05% sodium azide, and 0.1% Triton X-100) containing 10% horse serum for 30–45 min at 48C. The cells were washed and incubated with an anti-rabbit cortactinY421 primary antibody 1:100 dilution) in the blocking solution for 2 h at 4°C. The primary antibody was detected by the following incubation of a Cy2-conjugated secondary antibody (1:500 dilution) in blocking solution for 1–2 h at 4°C. Actin staining of the same cells stained for cortactinY421 was performed using rhodamine phalloidin (1:500 dilution) in PBS containing 5 mM EGTA (PBS–EGTA). The cells were rinsed by several changes of PBS–EGTA and mounted on a slide in a mounting solution (Vector Laboratories, Inc., Burlingame, CA). Immunostained osteoclasts were photographed with a Bio-Rad confocal laser-scanning microscope. Images were stored in TIF image format and processed by the Adobe Photoshop software program (Adobe System, Inc., Mountain View, CA).

Actin staining with rhodamine phalloidin

Osteoclasts were incubated on dentine slices for 18–24 h. Prior to staining, cells were washed three times with PBS–EGTA and fixed with 3.7% paraformaldehyde for 20 min at RT. Subsequently, cells were permeablized with 0.1% Triton X-100 for 5 min at RT and then washed three times with PBS–EGTA. Cells were stained with rhodamine phalloidin (1:500 dilution) for 30 min at RT or overnight at 4°C as described previously (Chellaiah et al., 1998, 2000b). Actin stained cells were viewed and photographed on a Bio-Rad confocal laser-scanning microscope. Images were stored in TIF image format and processed by the Adobe Photoshop software program (Adobe Systems, Inc.). Quantitative analysis of osteoclasts (~300–350) with actin rings after various treatments was performed at lower magnification with 20 × objective.

Measurement of F-actin content using rhodamine phalloidin binding

After various treatments as indicated in Figure 8, osteoclasts were rinsed with cold PBS and fixed with paraformaldehyde for 15 min, permeablized, and incubated with rhodamine phalloidin (1:200) in PBS for 30 min at 37°C. The cells were washed quickly several times with PBS and extracted with absolute methanol. The fluorescence of each sample was measured with fluorimetry (Bio-Rad spectrofluorometer). Osteoclasts untreated with rhodamine phalloidin were used to determine the background fluorescence of the cells. Empty wells without any cells were used to determine the non-specific binding. The non-

specific binding and background fluorescence was subtracted from the total binding to determine the specific binding (Cooper, 1992; Chellaiah and Hruska, 1996).

Bone resorption assay

Whale dentine slices (1.5 cm^2 across and 0.75 mm thick) were cut and processed as described previously (Chellaiah et al., 2000a). Cells transfected with Src (CA- and KD-Src) or PTP–PEST were scraped and plated after 36–48 h post-infection. Cells were scraped gently as explained above and the osteoclast suspension (2×10^4 cells) was added to each dentine slice. After 2 h of adherence,[C0]cells were treated for 48 h as indicated in Figure 7. Medium was replaced after 24 h with the respective treatment. After 48 h, cells were scraped-off from dentine, and the slices were washed twice with water. Pits were photographed under Bio-Rad confocal laser-scanning microscope. Images were stored in TIF image format and processed by the Adobe Photoshop software program (Adobe Systems, Inc.). Pit area was determined as described previously (Chellaiah et al., 2000a).

Data analysis

All values presented are expressed as the mean ± standard error of the mean (SEM) of three or more experiments done at different times and normalized to intra-experimental control values. Asterisks (*) and other symbols (·•, 0) were used to graphically indicate the statistical significance. A value of $P < 0.05$ was considered significant. For statistical comparisons, analysis of variance (ANOVA) was used with the Bonferroni corrections. Graph pad Instat (Graphpad Software, San Diego, CA) was used to perform the statistical tests.

Results

PTP–PEST regulates the phosphorylation state of Src at Y418

PTP–PEST has a regulatory role in the formation of sealing ring and podosomes (Chellaiah et al., 2001, 2007). Tyrosine phosphatase PTP-ε was shown to have a role in the activation of Src in osteoclasts (Gil-Henn and Elson, 2003). Reduced bone resorption and failure of sealing ring formation due to abnormal cytoskeletal reorganization in osteoclasts with reduced PTP–PEST levels (Chellaiah et al., 2007) prompted us to determine whether PTP–PEST has a role in the regulation of phosphorylation and activation of c-Src. Transfection of PTP–PEST SiRNA at dose of 1 μM for 36 h at 37°C reduced the endogenous protein levels of PTP–PEST by 70–80% (Fig. 1A, lane 2) as shown previously (Chellaiah et al., 2007). Untransfected or mock transfected (lane 1) and scrambled control SiRNA transfected (Sc; Fig. 1A, lane 3) cells were used as controls. Equal amounts of protein lysates (75 μg) were used for immunoblotting analyses with antibodies to Src Y527 (Fig. 1A, lanes 4–6) and Y418 (lanes 7–9). Dephosphorylation of Src at Y527 is critical for the unfolding and activation of c-Src by phosphorylation at Y418 in the catalytic site (Kaplan et al., 1994). An increase in the phosphorylation of Src at Y527 (lane 5) and a decrease at Y418 (lane 8) was observed in osteoclasts transfected with PTP–PEST SiRNA. Conversely, untransfected (lanes 4 and 7) and scrambled SiRNA transfected (Sc; lanes 6 and 9) osteoclasts resulted in effects opposite to those observed in SiRNA transfected cells (lanes 5 and 8). Immunoblotting with a GAPDH antibody shows approximate equal loading of proteins in

each lane (bottom parts; lanes 1–3 and 7–9). Reducing the levels of endogenous PTP–PEST has a negative influence on the activation of c-Src. These results suggest a possible role for PTP–PEST as a phosphotyrosine phosphatase (PTP) in the regulation of activation of c-Src.

To further elucidate the role of PTP–PEST in activating Src, osteoclasts were infected with adenovirus containing PTP–PEST cDNA (Fig. 1B, lane 4). PTP–PEST has been identified to modulate the phosphorylation state of Src at Y527 and Y418 (Fig. 1A). Therefore, concurrent infections were performed with adenovirus containing CA- (lane 1) and KD-Src (lane 2) constructs as controls to corroborate the effect of PTP–PEST. CA-Src contains a point mutation at aa527 (YΔF) to prevent tail binding to the SH2 domain. KD-Src contains two point mutations at aa297 (KΔR; to prevent ATP transfer) and aa527 (YΔF). More than two- to threefold as much Src (CA- and KD-Src; Fig. 1B, lanes 1 and 2) and PTP–PEST (lane 4) was noticeable in adenovirus-infected osteoclasts compared with the uninfected controls (lanes 3 and 5).

Subsequently, we determined the functional significance for the over-expression of PTP–PEST and c-Src (CA-and KD-Src) on the phosphorylation of c-Src at Y418 by immunoblotting with a phospho-specific antibody towards Src Y418 (Fig. 1C). An increase in the phosphorylation of Src at Y418 was observed in osteoclasts over-expressing PTP–PEST (Fig. 1C, lane 2) and CA-Src (lane 4). Src phosphorylation in osteoclasts expressing KD-Src (lane 3) was found to be below the control level (lane 1), although the expression level of this protein (Fig. 1D, lane 3) is equal to CA-Src (Fig. 1D, lane 4). The levels of total c-Src in control and PTP–PEST remained equal (Fig. 1D, lanes 1 and 2). The immunoblots were reprobed with an antibody to GAPDH to corroborate equal protein loading (bottom part in B and C). A change in the phosphorylation levels of Src at Y418 in osteoclasts with increased levels of PTP–PEST further substantiates its role in Src activation.

PTP–PEST increases phosphorylation of cortactin, Src, and WASP

Since cortactin is a substrate for c-Src, we subsequently proceeded to determine whether PTP–PEST expression will increase the phosphorylation of cortactin at Y421 (Fig. 2A).Equal amounts of protein lysates (100 μg) were immunoblotted with a phospho-specific antibody towards cortactinY421. An increase in the phosphorylation of cortactin was observed in cells over-expressing PTP–PEST and CA-Src proteins (Fig. 2A, lanes 2 and 4) as compared with the control (lane 1) and KD-Src expressing (lane 3) osteoclasts. The immunoblot was stripped and reprobed with a cortactin antibody to demonstrate that comparable amounts of protein were loaded in each lane (bottom part).

We have previously demonstrated that phosphorylation of WASP and WASP-associated proteins are increased in osteoclasts expressing CA-Src (Chellaiah et al., 2007). Lysates (100 μg protein) made from osteoclasts uninfected (control) or infected with adenovirus containing Src (CA- and KD-Src) and PTP–PEST constructs were immunoprecipitated with an antibody to WASP (lanes 1–4) or non-immune serum (NI, lane 5). As shown previously (Chellaiah et al., 2007), immunoblotting analysis with a monoclonal antibody to phosphotyrosine (4G10) demonstrated coprecipitation of phosphoproteins with apparent molecular weight of 60 kDa (c-Src) and 85 kDa (cortactin) (Fig. 2B). CA-Src increased the phosphorylation of WASP and cortactin (lane 2) as compared with KD-Src expressing (lane

1) and control (lane 3) osteoclasts. An increase in the phosphorylation of these proteins was also observed in osteoclasts over-expressing PTP–PEST (lane 4). Coimmunoprecipitation of Src and cortactin with WASP was confirmed by immunoblotting with respective antibodies in Figure 4 and previously (Chellaiah et al., 2007). The blot was then reprobed with the same WASP antibody after stripping to demonstrate the amount of WASP in each immunoprecipitate (bottom part in B). Taken together, this set of experiments showed that PTP–PEST has the ability to increase the phosphorylation of WASP and the associated Src and cortactin proteins. The effects observed in osteoclasts transfected with CA- and KD-Src serves as controls.

PTP–PEST increases dephosphorylation of Src at Y527 and activates it

Subsequently, we sought to demonstrate a biochemical mechanism by which PTP–PEST can regulate the activation of Src. As shown in Figure 1, dephosphorylation of Src at Y527 is critical for the unfolding and activation of c-Src by phosphorylation at Y418 in the catalytic site. Since PTP–PEST increases the phosphorylation of Src at Y418 (Fig. 1C), we analyzed the levels of Src phosphorylation at Y527 (Fig. 3). About 100 μg of protein lysates were immunoblotted with a phospho-specific antibody towards Src Y527 (Fig. 3A). Basal level phosphorylation of Src was observed at Y527 in osteoclasts uninfected (control; lanes 3 and 8) or infected with adenovirus containing constructs for PTP–PEST (lane 2), KD-Src (lane 6), and CA-Src (lane 7). Since CA- and KD-Src harbor mutations at 527(YΔF), very little tyrosine phosphorylation at Y527 was observed (lanes 6 and 7).

To further determine the relationship between Src phosphorylation and activation by PTP–PEST, control (Fig. 3A, lane 5) and PTP–PEST over-expressing (lane 1) osteoclasts were treated with a potent PTP inhibitor PAO (lane 1) as shown previously (Chellaiah et al., 2007). Since BPs inhibit tyrosine phosphatases (Opas et al., 1997), some cultures over-expressing PTP–PEST were also treated with alendronate (lane 4) (Samanna et al., 2007). A detectable increase in the phosphorylation of Src at Y527 in osteoclasts treated with PAO (Fig. 3A, lanes 1 and 5) and alendronate (lane 4) was observed. Immunoblotting analysis of the same blot with an Src antibody after stripping demonstrates the amount of Src in each lane (bottom part, lanes 1–8). An increase in the expression of Src (CA- and KD-Src) was observed after 48–72 h post-infection (lanes 6 and 7).

In order to substantiate that an increase in the phosphorylation of Src at Y527 corresponds with the decrease in the phosphorylation of Src at Y418 in PAO and alendronate-treated osteoclasts, immunoblotting was performed with an antibody to SrcY418 (Fig. 3B). As expected, PAO and alendronate diminished the phosphorylation of Src at Y418 (lanes 1–4) and activity towards phosphorylating cortactin (see Fig. 4) and WASP (data not shown). As a loading control, the blot was also probed with an antibody to GAPDH without stripping. Taken together, as alluded to above, results with PAO and alendronate strengthen our notion that PTP–PEST has a role in the activation of c-Src via modulating the phosphorylation state of Src at Y527.

Activation of Src by PTP–PEST increases cortactin phosphorylation and its association with WASP

We have previously demonstrated the coprecipitation of a protein with an apparent molecular weight of 85 kDa in SDS–PAGE with WASP (Chellaiah et al., 2007). Later this protein was confirmed as cortactin by immunoblotting analysis. Cortactin is a substrate for Src and phosphorylation of cortactin on Y421 is regulated by Src activity (Wu and Parsons, 1993; Tehrani et al., 2007). To examine the effect of PTP–PEST in the phosphorylation of cortactin and its interaction with WASP, lysates (500 μg protein) made from osteoclasts subjected to various treatments as indicated in Figure 4 were either immunoprecipitated with a WASP antibody (Fig. 4A, lanes 2–7) or pulldown with GST-fused GP domain of WASP (Fig. 4B, lanes 1–5). Immunoprecipitation with a non-immune serum (NI, lane 1 in Fig. 4A) or pulldown with GST alone (Fig. 4B, lane 6) was used as a negative control. Immunoblotting analysis was performed with a cortactinY421 antibody. An increase in the coprecipitation or pulldown of cortactin with WASP immunoprecipitates or GST/WASP-GP domain was observed in osteoclasts expressing PTP–PEST (Fig. 4A, lane 2; Fig. 4B, lane 1). The above finding is in agreement with our perception that PTP–PEST increases cortactin phosphorylation and its interaction with WASP via modulation of Src activity. PTP–PEST-induced cortactin phosphorylation is reduced by PAO and alendronate (Fig. 4A, lanes 4 and 6; Fig. 4B, lanes 3 and 5) to lower than basal level observed in control cells (Fig. 4A, lane 7; Fig. 4B, lane 2). A Src inhibitor PP2 displayed similar effects as that of PAO in the inhibition of phosphorylation of cortactin associated with WASP (Fig. 4A, lane 3). However, a remarkable inhibition of phosphorylation of cortactin was observed in osteoclasts treated with both PAO and PP2 (Fig. 4A, lane 5). This decrease was more than the one observed with alendronate (Fig. 4A, lane 6).

Subsequently, immunoblotting analysis with a cortactin antibody was performed (A and B, middle part). Cortactin levels associated with WASP or pulldown with GST-fused GP-domain of WASP match-up with the phosphorylation state of cortactin. From the immunoblotting analyses with a WASP (bottom part in A) and GST antibody (bottom part in B), we demonstrate that equal levels of proteins and GST-fused WASP-GP domain were used for the outcome described above. The GP domain of WASP corresponding to aa228–408 contains approximately six proline-rich clusters in aa311–404. A decrease in the pull down of cortactin in osteoclasts treated with PAO, PP2, and PAO/PP2 suggests that cortactin could have an affinity to the proline-rich region of WASP. It also suggests that the phosphorylation of cortactin on Y421 may perhaps be vital to this process. Taken together, our results demonstrate an increase in the phosphorylation of cortactin by PTP–PEST. A decrease in the effect of PTP–PEST by PP2 support that Src is activated by PTP–PEST.

Inhibition of PTP–PEST activity diminishes interaction of Arp2 with WASP

Cortactin and WASP synergistically regulate the Arp2/3-mediated actin filament branching (Weaver et al., 2001). The interactions of Arp2/3 complex with WASP, sealing ring formation, and bone resorption are increased in osteoclasts expressing constitutively active Rho GTPase (Rho^{val14}) (Chellaiah, 2005). Next, we analyzed the effects of various treatments on the interaction of WASP with Arp2 (Fig. 5). Lysates (500 mg protein) made from osteoclasts subjected to various treatments were either immunoprecipitated with a

WASP antibody (lanes 2–9) or a species-specific non-immune serum (NI, lane 1). Immunoblotting was performed with an Arp2 antibody. The blot was stripped and reprobed with a WASP antibody to detect the level of WASP in each of the immunoprecipitates (bottom part). An increase in WASP–Arp2 complex was found in osteoclasts expressing CA-Src and PTP–PEST (lanes 3 and 4). A dramatic decrease in the PTP–PEST induced WASP–Arp2 complex formation by PAO is comparable with the effects of alendronate and PP2 (top part; lanes 7–9). Since CA-Src has a mutation at Y527F, PAO had no effect on the CA-Src induced WASP–Arp2 complex formation (lane 5). However, a decrease in the formation of WASP–Arp2 complex in osteoclasts expressing CA-Src and treated with alendronate (lane 6) was observed. The precise molecular mechanism involved in this decrease remains unknown.

Inhibitors to Src kinase (PP2) and protein–tyrosine phosphatase (PAO) have equal effects as that of bisphosphonates

Effects of inhibitors (PAO and PP2) and alendronate on sealing ring formation and bone resorption.—As shown previously (Chellaiah et al., 2007), CA-Src increases sealing ring formation (Fig. 6) and bone resorption (Fig. 7). PTP–PEST also increases the number of actin rings (Fig. 6) and bone resorption in vitro (Fig. 7) to a level lesser than CA-Src and greater than control cells. Failure of formation of functional actin rings in osteoclasts transfected with PTP–PEST and then treated with PP2/PAO, PP2, PAO, or alendronate (Fig. 6) corresponds with reduced bone resorption in these osteoclasts (Fig. 7). A significant decrease in osteoclasts over-expressing PTP–PEST and treated with PAO/PP2 (G) reveals the significance of PTP–PEST and Src kinase in the regulation of phosphorylation state of proteins involved in sealing ring formation. Inhibition of sealing ring formation and bone resorption by inhibitors and alendronate was observed in the following order in PTP–PEST transfected cells; PAO/PP2 > PP2 > alendronate > PAO. Osteoclasts expressing CA-Src and treated with alendronate also displayed a significant decrease in the number of sealing rings (Fig. 6) and bone resorption (Fig. 7) although very minor effect was observed with PAO. This again accentuate that PTP–PEST is not a downstream regulator of Src. Although the precise mechanism is unknown, we propose the following: Alendronate inhibits Rho activation by preventing geranylgeranylation, which results in the inhibition of migration of human ovarian cancer cells (Sawada et al., 2002). We have previously demonstrated that Rho family proteins (Rho and Cdc42) play a crucial role in WASP activation and interaction of Arp2/3 with WASP (Chellaiah, 2005). A decrease in the formation of WASP–Arp2 complex (Fig. 5) and the number of actin rings in osteoclasts treated with alendronate (Fig. 6) indicate the possibility that it may block Rho family proteins-mediated WASP activation, WASP–Arp2/3 complex formation, and actin polymerization.

Localization of cortactinY421/actin in sealing ring of resorbing osteoclasts and measurement of F-actin content.—Inhibition of WASP–Arp2 complex (Fig. 5) as well as sealing ring formation (Fig. 6) and bone resorption (Fig. 7) by alendronate and not by PAO in CA-Src transfected cells prompted us to confirm that the impairment of sealing ring formation is due to the inhibition of Src activity or a result of the failure of cytoskeletal regulation independent of Src activity. Given the role of Src in cortactin phosphorylation on

Y421 as shown in Figure 2 and its role in actin assembly in osteoclasts (Tehrani et al., 2007), we analyzed the localization of phosphocortactin Y421 and actin in resorbing osteoclasts transfected with CA-Src (Fig. 8A). Colocalization (yellow) of cortactinY421 (green) and actin (red) was observed in the sealing ring of CA-Src transfected and PBS-treated control osteoclasts. These osteoclasts demonstrated diffuse distribution of cortactinY421 through out the cytoplasm. Since CA-Src has mutation at Y527F, PAO or alendronate had no effect on the Src activity. Therefore, phosphorylation state or diffuse distribution of cortactinY421 is very similar to PBS-treated osteoclasts. Further more, sealing ring formation or colocalization of cortactinY421 and actin are unaffected in PAO-treated osteoclasts. However, inhibition of sealing ring formation and a decrease in actin staining in alendronate-treated osteoclasts suggests that a signaling pathway involved in actin assembly is blocked by alendronate independent of Src effect.

Subsequently, we proceeded to examine the effects of various treatments on the F-actin content in osteoclasts (Fig. 8). As shown previously (Chellaiah et al., 2007), an increase in F-actin content was observed in osteoclasts transfected with CA-Src and PTP–PEST as compared with KD-Src transfected and control untransfected cells (Fig. 8B). F-actin content is significantly reduced in osteoclasts transfected with PTP–PEST and followed by treatment with alendronate, pamidronate, PAO, PP2, and PAO/PP2 (Fig. 8C). In CA-Src-transfected cells, alendronate and PP2 significantly decreased the F-actin content although PAO had a very negligible effect. Taken together, we have shown here that PTP–PEST regulates Src activity and osteoclast function. Inhibition of either one of them (PTP–PEST or Src) by PAO or PP2 could block osteoclast sealing ring formation and bone resorption. Also, these inhibitors displayed more or less equal effects as that of BPs in osteoclast function (Figs. 6–8); however, jointly PAO/PP2 is more effective than BPs (Figs. 6, 7, and 8C).

Discussion

Sealing ring formation is fundamental to the process of osteoclast bone resorption. Src is a critical regulator of osteoclast bone resorption and Src null osteoclasts failed to form ruffled border and could not resorb bone. Therefore, Src null mice develop osteopetrosis (Boyce et al., 1992; Miyazaki et al., 2006). The principal molecular mechanism(s) by which Src kinase phosphorylation is regulated and activated is (are) largely unknown. Protein phosphorylation is regulated by protein kinases and phosphatases. Several phosphatases (PTPRO, PTP-epsilon, SHP-1, and PTP–PEST) have been shown to regulate the function of osteoclasts (Puzas and Brand, 1985; Schmidt et al., 1996; Chellaiah et al., 2001, 2007; Takeshita et al., 2002; Amoui et al., 2003; Gupta et al., 2003; Chiusaroli et al., 2004; Lau et al., 2006; Granot-Attas and Elson, 2008; reviewed in Granot-Attas et al., 2007). Previous studies from our laboratory demonstrated that PTP–PEST associates with actin regulatory or actin binding proteins (gelsolin, leupaxin, and WASP) and regulates podosome assembly/disassembly and sealing ring formation (Chellaiah et al., 2001, 2007; Gupta et al., 2003). However, the exact role of PTP–PEST and the precise mechanism by which it regulates the signaling molecules involved in cytoskeletal remodeling is not known. It was expected that reducing the levels of PTP–PEST would increase the kinase activity and osteoclast function. However, we have previously shown that SiRNA to PTP–PEST reduced actin ring formation and bone resorption (Chellaiah et al., 2007). Here we have shown that SiRNA to PTP–PEST

inhibit the phosphorylation of Src at Y527 (Fig. 1A). Based on these observations we hypothesized that over-expression of PTP–PEST will augment kinase activity and PTP–PEST activity is indispensable for the activation of Src and its downstream effects. The data presented here supports our hypothesis that PTP–PEST activates Src via dephosphorylating it at Y527 (Tyr530 in human c-Src equivalent to Tyr527 in chicken Src). PAO, a potent protein–tyrosine phosphatase (PTP) inhibitor reduced the dephosphorylation state at Y527 to a greater extent and decreased the activation of Src due to decreased phosphorylation at Y418 (Fig. 3). Candidate phosphotyrosine 527 phosphatases list include cytoplasmic enzymes PTP1B, SHP1 and SHP 2, and transmembrane enzymes CD45, PTP-alpha (α), PTP-epsilon (ε), PTP-lambda (λ), and PTP-oc (Amoui et al., 2003; Roskoski, 2005). However, PTP–PEST has not been listed as one among them. Our observations suggest PTP–PEST is an important regulator of SrcY527 in osteoclasts and it could now be included to the list of phosphotyrosine 527 phosphatases.

Studies performed with osteoclasts that over-express PTP–PEST or are treated with a potent PTP inhibitor PAO reveal an intriguing pathway. It shows that the phosphorylation of Src at Y418 is regulated by the dephosphorylation of Src at Y527 by PTP–PEST. Osteoclasts transfected with CA-Src and treated with an Src kinase inhibitor PP2 simulate the effects of PAO in PTP–PEST transfected cells (Figs. 4–8). We believe that the ability of PTP–PEST to activate Src is corroborated by the effects observed with PP2 treatment in osteoclasts expressing PTP–PEST (Figs. 4–8). Enhanced phosphorylation of Src at Y418, cortactin at Y421, and WASP at Y291 (Figs. 1–3) as well as an increase in the number of sealing rings and bone resorption (Figs. 6 and 7) in PTP–PEST transfected osteoclasts suggest that PTP–PEST may serve to regulate Src activity, which has been shown extensively as a key regulator of osteoclast function (Boyce et al., 1992; Tanaka et al., 1992; Chellaiah et al., 1998; Violette et al., 2000; Zou et al., 2007; reviewed in Baron, 1996).

The possible role of PTP–PEST in osteoclast sealing ring formation and bone resorption is summarized in the scheme provided in Figure 9. The inhibition of PTP–PEST activity by PAO not only reduced the phosphorylation state of Src at Y418 but also the downstream effects of Src in the phosphorylation of cortactin, WASP (Fig. 4), as well as interaction of WASP with Arp2 (Fig. 5). Coprecipitation of cortactin (Fig. 4) and Arp2 (Fig. 5) with WASP, and increased phosphorylation of both cortactin and WASP (Fig. 2) in osteoclasts transfected with CA-Src and PTP–PEST suggests that WASP Arp2 cortactin complex (Figs. 4 and 5) play a part in actin dynamics during sealing ring formation. WASP can integrate signals from Src, PTP–PEST, and other kinases in order to regulate the remodeling of cytoskeleton during bone resorption (Chellaiah, 2005; Chellaiah et al., 2007). Tyrosine phosphorylation of WASP at Y291 was found to be an important regulatory event in the function of WASP. Transduction of WASP peptide containing Y291 aa not only blocked the phosphorylation of endogenous WASP at Y291 but also its interaction with Arp2 or 3, formation of sealing ring and bone resorption (Ma et al., 2008).

A number of proteins have been identified to interact with or activate WASP in osteoclasts and other cell systems (Banin et al., 1996b; Wu et al., 1998; Schulte and Sefton, 2003; Chellaiah, 2006; Torres and Rosen, 2006; Chellaiah et al., 2007). WASP and cortactin can simultaneously bind Arp2/3 and synergistically enhance the Arp2/3-induced actin filament

branching (Weaver et al., 2002). Cortactin contains SH3 domain at the C-terminal region (aa327–546) and it interacts with proline-rich sequences of actin regulatory proteins such as, N-WASP, WASP-interacting protein (WIP), and dynamin through this domain (Kinley et al., 2003; McNiven et al., 2004; Kowalski et al., 2005). Coprecipitation of cortactin with the GP-domain of WASP suggests that cortactin may be a direct binding partner of WASP (Fig. 4A). Pulldown analysis (Fig. 4B) suggests that cortactin may interact with WASP-GP-domain via SH3 domain. GP domain of WASP consists of six proline-rich amino acids between residues 311 and 404. We have previously demonstrated pulldown of multiple proteins (Src, PTP–PEST, 160 kD protein characterized as Rho kinase, and PSTPIP) with GST-fused WASP-GP domain besides cortactin. It is possible that these proteins may either interact with each other through modular domains or have specificity to different proline-rich sequences within the GP-domain of WASP.

Over-expression of either full-length cortactin or cortactin C-terminus containing SH3 domain enhances migration of mammary epithelial cells (Kowalski et al., 2005). Our recent experiments with SiRNA to cortactin exhibited a significant decrease in the interaction of WASP with Arp2/3 complex, formation of sealing ring, and bone resorption in osteoclasts (data not shown). Cortactin depletion by RNA interference in osteoclasts led to a specific loss of podosomes on non-osteoid surface (coverslips). It also displayed complete loss of bone resorption with no formation of sealing zones on osteoid surfaces (bone) (Tehrani et al., 2006). WASP was identified as a critical regulator of sealing formation. Failure of sealing ring formation in osteoclasts from WASP null mice (Calle et al., 2004) or in osteoclasts treated with SiRNA to WASP (Chellaiah, 2005) suggests that WASP has a direct role in actin polymerization and may be a direct activator of Arp2/3 complex.

Nevertheless, we cannot exclude the possibility that both cortactin and WASP are critical regulators of sealing ring formation. From our current observations, we propose that there could be a number of ways through which cortactin may assist in actin polymerization in conjunction with WASP: (a) cortactin may be an upstream regulator or mediator of actin polymerization through WASP. (b) Cortactin may be associated with WASP and engaged in actin polymerization in a manner dependent on phosphorylation of its tyrosine residues by Src. (c) Cortactin may assist in the stabilization of WASP through its binding to the proline-rich region and maintain it in the active state as shown by others (Kowalski et al., 2005). (d) Interaction of cortactin with WASP intensifies the effects of Arp2/3 complex in actin polymerization and sealing ring formation as depletion of cortactin reduces Arp2/3 interaction with WASP (data not shown). (e) Both WASP and cortactin works jointly and deletion of either one encumbers sealing ring formation. We concluded here that regulation of phosphorylation and activation of Src kinase by PTP–PEST plays a role in the phosphorylation of proteins associated with actin dynamics and sealing ring formation (see schematic Fig. 9).

Patients with osteoporosis, breast cancer, prostate cancer, and multiple myeloma are treated with BPs to reduce or delay skeletal events (Lipton, 2004). Alendronate has an effect on the activity of phosphatases, disruption of actin ring structure, and inhibition of kinase activation in osteoclasts (Schmidt et al., 1996; Opas et al., 1997; Fisher et al., 1999). Since the over-expression of PTP–PEST in osteoclasts is linked to kinase activation with phosphatase

activity (Figs. 1–3), we further analyzed the effects of alendronate on Src activation. As demonstrated previously (Samanna et al., 2007), both alendronate and pamidronate (data not shown) produced similar effects in the inhibition of PTP–PEST and sealing ring formation. The inhibition of Src activation by alendronate in cells over-expressing PTP–PEST suggests that it is a molecular target for alendronate.

As shown by others, inhibition of actin ring formation in alendronate-treated osteoclasts expressing CA-Src (Fig. 8) suggests that Rho GTPases are also targets for BPs (Rogers et al., 2000; Rogers, 2003). In addition, Rho family GTPases play a critical role in the formation of cortical actin networks in mammalian cells (Weed et al., 2000). Although, cortactin is phosphorylated on Y421 (Fig. 8) and has a domain for F-actin and Arp2/3 binding, it is not able to execute actin assembly independently, because the translocation of cortactin to cell periphery requires Rho family members (Weed et al., 1998). Cortactin and WASP presumably function in cortical cytoskeletal rearrangements by actin nucleation and thereby can induce the formation of a branched cortical actin network in the process of sealing ring assembly.

Since spatio-temporal localization of cortactin is critical in actin assembly and sealing ring formation, it will be interesting to elucidate the manner in which cortactin (either domains or phosphorylation events of cortactin) regulates cytoskeletal rearrangement jointly with WASP in osteoclasts. Osteoclasts transfected with PTP–PEST and subsequently treated with PAO, PP2, or alendronate demonstrated relatively equal inhibitory effects in sealing ring formation, bone resorption, and actin polymerization (Figs. 4–8). BPs are used to treat, delay/prevent, or reverse bone loss associated with osteoporosis, cancer metastasis, and other bone loss disorders. Due to the promising effects of inhibitors to phosphatase and kinase and given that the effects are equal to BPs (alendronate and pamidronate); we will explore the biochemical and cell biological effects of different BPs and other similar compounds.

Acknowledgments

This work was supported by the National Institute of Health Grant R01-AR46292 (to M.A.C.). We thank Dr. Michael Roger (Institute of Medical Sciences, University of Aberdeen, Aberdeen AB25 2ZD, UK) for bisphosphonates (alendronate and pamidronate); Dr. Dhandapani Kuppuswamy (Gazes Cardiac Research Institute, Cardiology Division, Medical University of South Carolina, Charleston, South Carolina 29425) for adenoviral Src constructs (CA- and KD- Src); Dr. Stefan Linder (Institut fuer Prophylaxe und Epidemiologie der Kreislaufkrankheiten, Ludwig-Maximilians-Universitaet, Pettenkoferstrasse 9, D-80336 Muenchen, Germany) for GST-fused WASP-GP domain; Dr. Arasu Chellaiah for proofreading the manuscript.

Contract grant sponsor: National Institutes of Health; Contract grant number: R01-AR46292.

Abbreviations:

Al	alendronate
Arp 2	Actin related protein 2
CA-Src	constitutively active-Src
F-actin	filamentous actin
GST	glutathione S-transferase

GP domain	GBD and proline-rich domain
GAPDH	glyceraldehyde-3-phosphate dehydrogenase
HRP	horse radish peroxide
KD-Src	kinase-defective-Src
mCSF-1	macrophage colony stimulating factor
a-MEM	minimum Eagle's a-medium
NI	non-immune serum
PAO	phenyl arsine oxide; PBS, phosphate-buffered saline
PSTPIP	proline-, serine, threonine rich phosphatase-interacting protein
PTP–PEST	protein-tyrosine phosphatase-proline, glutamic acid, serine, threonine amino acid sequences
Src inhibitor PP2	(4-amino-5-(4-chloro-phenyl)-7-(t-butyl) pyrazolo [3,4-d] pyrimidine)
PVDF	polyvinyldifluoride
RANK-L	receptor activator of nuclear factor kappa B ligand
WASP	Wiskott–Aldrich syndrome protein

Literature Cited

Amoui M, Baylink DJ, Tillman JB, Lau KH. 2003 Expression of a structurally unique osteoclastic protein-tyrosine phosphatase is driven by an alternative intronic, cell type-specific promoter. J Biol Chem 278:44273–44280. [PubMed: 12949066]

Badour K, Zhang J, Shi F, Leng Y, Collins M, Siminovitch KA. 2004 Fyn and PTP-PEST-mediated regulation of Wiskott-Aldrich syndrome protein (WASp) tyrosine phosphorylation is required for coupling T cell antigen receptor engagement to WASp effector function and T cell activation. J Exp Med 199:99–112. [PubMed: 14707117]

Banin S, Truong O, Katz DR, Waterfield MD, Brickell PM, Gout I. 1996a Wiskott-Aldrich syndrome protein (WASp) is a binding partner for c-Src family protein-tyrosine kinases. Curr Biol 6:981–988. [PubMed: 8805332]

Banin S, Truong O, Katz DR, Waterfield MD, Brickell PM, Gout I. 1996b Wiskott-Aldrich syndrome protein (WASp) is a binding partner for c-Src family protein-tyrosine kinases. Curr Biol 6:981–988. [PubMed: 8805332]

Baron R. 1996 Molecular mechanisms of bone resorption: Therapeutic implications. Rev Rhum Engl Ed 63:633–638. [PubMed: 8953663]

Boyce BF, Yoneda T, Lowe C, Soriano P, Mundy GR. 1992 Requirement of pp60c-src expression for osteoclasts to form ruffled borders and resorb bone in mice. J Clin Invest 90:1622–1627. [PubMed: 1383278]

Calle Y, Jones GE, Jagger C, Fuller K, Blundell MP, Chow J, Chambers T, Thrasher AJ. 2004 WASp deficiency in mice results in failure to form osteoclast sealing zones and defects in bone resorption. Blood 103:3552–3561. [PubMed: 14726392]

Chellaiah MA. 2005 Regulation of actin ring formation by RhoGTPases in osteoclasts. J Biol Chem 280:32930–32943. [PubMed: 16006560]

Chellaiah MA. 2006 Regulation of podosomes by integrin alphavbeta3 and Rho GTPase-facilitated phosphoinositide signaling. Eur J Cell Biol 85:311–317. [PubMed: 16460838]

Chellaiah M, Hruska KA. 1996 Osteopontin stimulates gelsolin associated phosphoinositide levels and PtdIns 3-hydroxyl kinase. Mol Biol Cell 7:743–753. [PubMed: 8744948]

Chellaiah M, Fitzgerald C, Alvarez U, Hruska K. 1998 C-src is required for stimulation of gelsolin associated PI3-K. J Biol Chem 273:11908–11916. [PubMed: 9565618]

Chellaiah M, Kizer N, Silva M, Alvarez U, Kwiatkowski D, Hruska KA. 2000a Gelsolin deficiency blocks podosome assembly and produces increased bone mass and strength. J Cell Biol 148:665–678. [PubMed: 10684249]

Chellaiah M, Soga N, Swanson S, McAllister S, Alvarez U, Wang D, Dowdy SF, Hruska KA. 2000b Rho-A is critical for osteoclast podosome organization, motility, and bone resorption. J Biol Chem 275:11993–12002. [PubMed: 10766830]

Chellaiah MA, Biswas RS, Yuen D, Alvarez UM, Hruska KA. 2001 Phosphatidylinositol 3,4,5-trisphosphate directs association of Src homology 2-containing signaling proteins with gelsolin. J Biol Chem 276:47434–47444. [PubMed: 11577104]

Chellaiah MA, Kizer N, Biswas R, Alvarez U, Strauss-Schoenberger J, Rifas L, Rittling SR, Denhardt DT, Hruska KA. 2003 Osteopontin deficiency produces osteoclast dysfunction due to reduced CD44 surface expression. Mol Biol Cell 14:173–189. [PubMed: 12529435]

Chellaiah MA, Kuppuswamy D, Lasky L, Linder S. 2007 Phosphorylation of a Wiscott-Aldrich syndrome protein-associated signal complex is critical in osteoclast bone resorption. J Biol Chem 282:10104–10116. [PubMed: 17283076]

Chiusaroli R, Knobler H, Luxenburg C, Sanjay A, Granot-Attas S, Tiran Z, Miyazaki T, Harmelin A, Baron R, Elson A. 2004 Tyrosine phosphatase epsilon is a positive regulator of osteoclast function in vitro and in vivo. Mol Biol Cell 15:234–244. [PubMed: 14528021]

Cooper JA. 1992 Actin filament assembly and organization in vitro In: Carraway KL, Carraway CAC, editors. The cytoskeleton: A practical approach. New York: Oxford University Press pp 47–71.

Cory GOC, Cramer R, Blanchoin L, Ridley AJ. 2003 Phosphorylation of the WASP-VCA domain increases its affinity for the Arp2/3 complex and enhances actin polymerization by WASP. Mol Cell 11:1229–1239. [PubMed: 12769847]

Cote JF, Charest A, Wagner J, Tremblay ML. 1998 Combination of gene targeting and substrate trapping to identify substrates of protein tyrosine phosphatases using PTP-PEST as a model. Biochemistry 37:13128–13137. [PubMed: 9748319]

Duncan RL, Kizer N, Barry ELR, Friedman PA, Hruska KA. 1996 Antisense oligodeoxynucleotide inhibition of a swelling-activated cation channel in osteoblast-like osteosarcoma cells. Proc Natl Acad Sci USA 93:1864–1869. [PubMed: 8700850]

Dunford JE, Thompson K, Coxon FP, Luckman SP, Hahn FM, Poulter CD, Ebetino FH, Rogers MJ. 2001 Structure-activity relationships for inhibition of farnesyl diphosphate synthase in vitro and inhibition of bone resorption in vivo by nitrogen-containing bisphosphonates. J Pharmacol Exp Ther 296:235–242. [PubMed: 11160603]

Duong LT, Lakkakorpi PT, Nakamura I, Machwate M, Nagy RM, Rodan GA. 1998 PYK2 in osteoclasts is an adhesion kinase, localized in the sealing zone, activated by ligation of a_Vb_3 integrin, and phosphorylated by Src kinase. J Clin Invest 102:881–892. [PubMed: 9727056]

Endo N, Rutledge SJ, Opas EE, Vogel R, Rodan GA, Schmidt A. 1996 Human protein tyrosine phosphatase-sigma: Alternative splicing and inhibition by bisphosphonates. J Bone Miner Res 11:535–543. [PubMed: 8992885]

Fisher JE, Rogers MJ, Halasy JM, Luckman SP, Hughes DE, Masarachia PJ, Wesolowski G, Russell RG, Rodan GA, Reszka AA. 1999 Alendronate mechanism of action: Geranylgeraniol, an intermediate in the mevalonate pathway, prevents inhibition of osteoclast formation, bone resorption, and kinase activation in vitro. Proc Natl Acad Sci USA 96:133–138. [PubMed: 9874784]

Garton AJ, Tonks NK. 1994 PTP-PEST: A protein tyrosine phosphatase regulated by serine phosphorylation. EMBO J 13:3763–3771. [PubMed: 7520867]

Garton AJ, Tonks NK. 1999 Regulation of fibroblast motility by the protein tyrosine phosphatase PTP-PEST. J Biol Chem 274:3811–3818. [PubMed: 9920935]

Gil-Henn H, Elson A. 2003 Tyrosine phosphatase-epsilon activates Src and supports the transformed phenotype of Neu-induced mammary tumor cells. J Biol Chem 278:15579–15586. [PubMed: 12598528]

Granot-Attas S, Elson A. 2008 Protein tyrosine phosphatases. in osteoclast differentiation, adhesion, and bone resorption. Eur J Cell Biol 87:479–490. [PubMed: 18342392]

Granot-Attas S, Knobler H, Elson A. 2007 Protein tyrosine phosphatases in osteoclasts. Crit Rev Eukaryot Gene Expr 17:49–71. [PubMed: 17341183]

Gupta A, Lee BS, Khadeer MA, Tang Z, Chellaiah M, Abu-Amer Y, Goldknopf J, Hruska KA. 2003 Leupaxin is a critical adaptor protein in the adhesion zone of the osteoclast. J Bone Miner Res 18:669–685. [PubMed: 12674328]

He TC, Zhou S, da Costa LT, Yu J, Kinzler KW, Vogelstein B. 1998 A simplified system for generating recombinant adenoviruses. Proc Natl Acad Sci USA 85:2509–2514.

Kaplan KB, Bibbins KB, Swedlow JR, Arnaud M, Morgan DO, Varmus HE. 1994 Association of the amino-terminal half of c-Src with focal adhesions alters their properties and is regulated by phosphorylation of tyrosine 527. EMBO J 13:4745–4756. [PubMed: 7525268]

Kinley AW, Weed SA, Weaver AM, Karginov AV, Bissonette E, Cooper JA, Parsons JT. 2003 Cortactin interacts with WIP in regulating Arp2/3 activation and membrane protrusion. Curr Biol 13:384–393. [PubMed: 12620186]

Kowalski JR, Egile C, Gil S, Snapper SB, Li R, Thomas SM. 2005 Cortactin regulates cell migration through activation of N-WASP. J Cell Sci 118:79–87. [PubMed: 15585574]

Lau KH, Wu LW, Sheng MH, Amoui M, Suhr SM, Baylink DJ. 2006 An osteoclastic protein-tyrosine phosphatase is a potential positive regulator of the c-Src protein-tyrosine kinase activity: A mediator of osteoclast activity. J Cell Biochem 97:940–955. [PubMed: 16267838]

Linder S, Nelson D, Weiss M, Aepfelbacher M. 1999 Wiskott-Aldrich syndrome protein regulates podosomes in primary human macrophages. Proc Natl Acad Sci USA 96:9648–9653. [PubMed: 10449748]

Lipton A. 2004 Pathophysiology of bone metastases: How this knowledge may lead to therapeutic intervention. J Support Oncol 2:205–213. [PubMed: 15328823]

Ma T, Samanna V, Chellaiah MA. 2008 Dramatic inhibition of osteoclast sealing ring formation and bone resorption in vitro by a WASP-peptide containing pTyr294 amino acid. J Mol Signal 3:1–12. [PubMed: 18171471]

McNiven MA, Baldassarre M, Buccione R. 2004 The role of dynamin in the assembly and function of podosomes and invadopodia. Front Biosci 9:1944–1953. [PubMed: 14977600]

Miyazaki T, Tanaka S, Sanjay A, Baron R. 2006 The role of c-Src kinase in the regulation of osteoclast function. Mod Rheumatol 16:68–74. [PubMed: 16633924]

Moller NP, Moller KB, Lammers R, Kharitonenkov A, Sures I, Ullrich A. 1994 Src kinase associates with a member of a distinct subfamily of protein-tyrosine phosphatases containing an ezrin-like domain. Proc Natl Acad Sci USA 91:7477–7481. [PubMed: 7519780]

Murakami H, Takahashi N, Sasaki T, Udagawa N, Tanaka S, Nakamura I, Zhang D, Barbier A, Suda T. 1995 A possible mechanism of the specific action of bisphosphonates on osteoclasts: Tiludronate preferentially affects polarized osteoclasts having ruffled borders. Bone 17:137–144. [PubMed: 8554921]

Opas EE, Rutledge SJ, Golub E, Stern A, Zimolo Z, Rodan GA, Schmidt A. 1997 Alendronate inhibition of protein-tyrosine-phosphatase-meg1. Biochem Pharmacol 54:721–727. [PubMed: 9310349]

Playford MP, Lyons PD, Sastry SK, Schaller MD. 2006 Identification of a filamin docking site on PTP-PEST. J Biol Chem 281:34104–34112. [PubMed: 16973606]

Puzas JE, Brand JS. 1985 Bone cell phosphotyrosine phosphatase: Characterization and regulation by calcitropic hormones. Endocrinology 116:2463–2468. [PubMed: 2581772]

Rogers MJ. 2003 New insights into the molecular mechanisms of action of bisphosphonates. Curr Pharm Des 9:2643–2658. [PubMed: 14529538]

Rogers MJ, Gordon S, Benford HL, Coxon FP, Luckman SP, Monkkonen J, Frith JC. 2000 Cellular and molecular mechanisms of action of bisphosphonates. Cancer 88:2961–2978. [PubMed: 10898340]

Roskoski R Jr. 2005 Src kinase regulation by phosphorylation and dephosphorylation. Biochem Biophys Res Commun 331:1–14. [PubMed: 15845350]

Samanna V, Ma T, Mak TW, Rogers M, Chellaiah MA. 2007 Actin polymerization modulates CD44 surface expression, MMP-9 activation, and osteoclast function. J Cell Physiol 213:710–720. [PubMed: 17508356]

Sanjay A, Miyazaki T, Itzstein C, Purev E, Horne WC, Baron R. 2006 Identification and functional characterization of an Src homology domain 3 domain-binding site on Cbl. FEBS J 273:5442–5456. [PubMed: 17094785]

Sawada K, Morishige K, Tahara M, Kawagishi R, Ikebuchi Y, Tasaka K, Murata Y. 2002 Alendronate inhibits lysophosphatidic acid-induced migration of human ovarian cancer cells by attenuating the activation of rho. Cancer Res 62:6015–6020. [PubMed: 12414621]

Schmidt A, Rutledge SJ, Endo N, Opas EE, Tanaka H, Wesolowski G, Leu CT, Huang Z, Ramachandaran C, Rodan SB, Rodan GA. 1996 Protein-tyrosine phosphatase activity regulates osteoclast formation and function: Inhibition by alendronate. Proc Natl Acad Sci USA 93:3068–3073. [PubMed: 8610169]

Schulte RJ, Sefton BM. 2003 Inhibition of the activity of SRC and Abl tyrosine protein kinases by the binding of the Wiskott-Aldrich syndrome protein. Biochemistry 42:9424–9430. [PubMed: 12899629]

Takeshita S, Namba N, Zhao JJ, Jiang Y, Genant HK, Silva MJ, Brodt MD, Helgason CD, Kalesnikoff J, Rauh MJ, Humphries RK, Krystal G, Teitelbaum SL, Ross FP. 2002 SHIP-deficient mice are severely osteoporotic due to increased numbers of hyper-resorptive osteoclasts. Nat Med 8:943–949. [PubMed: 12161749]

Tanaka S, Takahashi N, Udagawa N, Sasaki T, Fukui Y, Kurokawa T, Suda T. 1992 Osteoclasts express high levels of p60c-src, preferentially on ruffled border membranes. FEBS Lett 313:85–89. [PubMed: 1385221]

Tehrani S, Faccio R, Chandrasekar I, Ross FP, Cooper JA. 2006 Cortactin has an essential and specific role in osteoclast actin assembly. Mol Biol Cell 17:2882–2895. [PubMed: 16611741]

Tehrani S, Tomasevic N, Weed S, Sakowicz R, Cooper JA. 2007 Src phosphorylation of cortactin enhances actin assembly. Proc Natl Acad Sci USA 104:11933–11938. [PubMed: 17606906]

Torres E, Rosen MK. 2006 Protein-tyrosine kinase and GTPase signals cooperate to phosphorylate and activate Wiskott-Aldrich syndrome protein (WASP)/neuronal WASP. J Biol Chem 281:3513–3520. [PubMed: 16293614]

Valleala H, Hanemaaijer R, Mandelin J, Salminen A, Teronen O, Monkkonen J, Konttinen YT. 2003 Regulation of MMP-9 (gelatinase B) in activated human monocyte/macrophages by two different types of bisphosphonates. Life Sci 73:2413–2420. [PubMed: 12954450]

Violette SM, Shakespeare WC, Bartlett C, Guan W, Smith JA, Rickles RJ, Bohacek RS, Holt DA, Baron R, Sawyer TK. 2000 A Src SH2 selective binding compound inhibits osteoclast-mediated resorption. Chem Biol 7:225–235. [PubMed: 10712930]

Virtanen SS, Vaananen HK, Harkonen PL, Lakkakorpi PT. 2002 Alendronate inhibits invasion of PC-3 prostate cancer cells by affecting the mevalonate pathway. Cancer Res 62:2708–2714. [PubMed: 11980672]

Weaver AM, Karginov AV, Kinley AW, Weed SA, Li Y, Parsons JT, Cooper JA. 2001 Cortactin promotes and stabilizes Arp2/3-induced actin filament network formation. Curr Biol 11:370–374. [PubMed: 11267876]

Weaver AM, Heuser JE, Karginov AV, Lee WL, Parsons JT, Cooper JA. 2002 Interaction of cortactin and N-WASp with Arp2/3 complex. Curr Biol 12:1270–1278. [PubMed: 12176354]

Weed SA, Du Y, Parsons JT. 1998 Translocation of cortactin to the cell periphery is mediated by the small GTPase Rac1. J Cell Sci 111:2433–2443. [PubMed: 9683637]

Weed SA, Karginov AV, Schafer DA, Weaver AM, Kinley AW, Cooper JA, Parsons JT. 2000 Cortactin localization to sites of actin assembly in lamellipodia requires interactions with F-actin and the Arp2/3 complex. J Cell Biol 151:29–40. [PubMed: 11018051]

Willey CD, Balasubramanian S, Rodriguez Rosas MC, Ross RS, Kuppuswamy D. 2003 Focal complex formation in adult cardiomyocytes is accompanied by the activation of beta3 integrin and c-Src. J Mol Cell Cardiol 35:671–683. [PubMed: 12788385]

Wu H, Parsons JT. 1993 Cortactin, an 80/85-kilodalton pp60src substrate, is a filamentous actin-binding protein enriched in the cell cortex. J Cell Biol 120:1417–1426. [PubMed: 7680654]

Wu Y, Dowbenko D, Lasky LA. 1998 PSTPIP 2, a second tyrosine phosphorylated, cytoskeletal-associated protein that binds a PEST-type protein-tyrosine phosphatase. J Biol Chem 273:30487–30496. [PubMed: 9804817]

Zhang D, Udagawa N, Nakamura I, Murakami H, Saito S, Yamasaki K, Shibasaki Y, Morij N, Narumiya S, Takahashi N, Suda T. 1995 The small GTP-binding protein, rho p21, is involved in bone resorption by regulating cytoskeletal organization in osteoclasts. J Cell Sci 108:2285–2292. [PubMed: 7673348]

Zhu S, Bjorge JD, Fujita DJ. 2007 PTP1B contributes to the oncogenic properties of colon cancer cells through Src activation. Cancer Res 67:10129–10137. [PubMed: 17974954]

Zou W, Kitaura H, Reeve J, Long F, Tybulewicz VL, Shattil SJ, Ginsberg MH, Ross FP, Teitelbaum SL. 2007 Syk, c-Src, the alphavbeta3 integrin, and ITAM immunoreceptors, in concert, regulate osteoclastic bone resorption. J Cell Biol 176:877–888. [PubMed: 17353363]

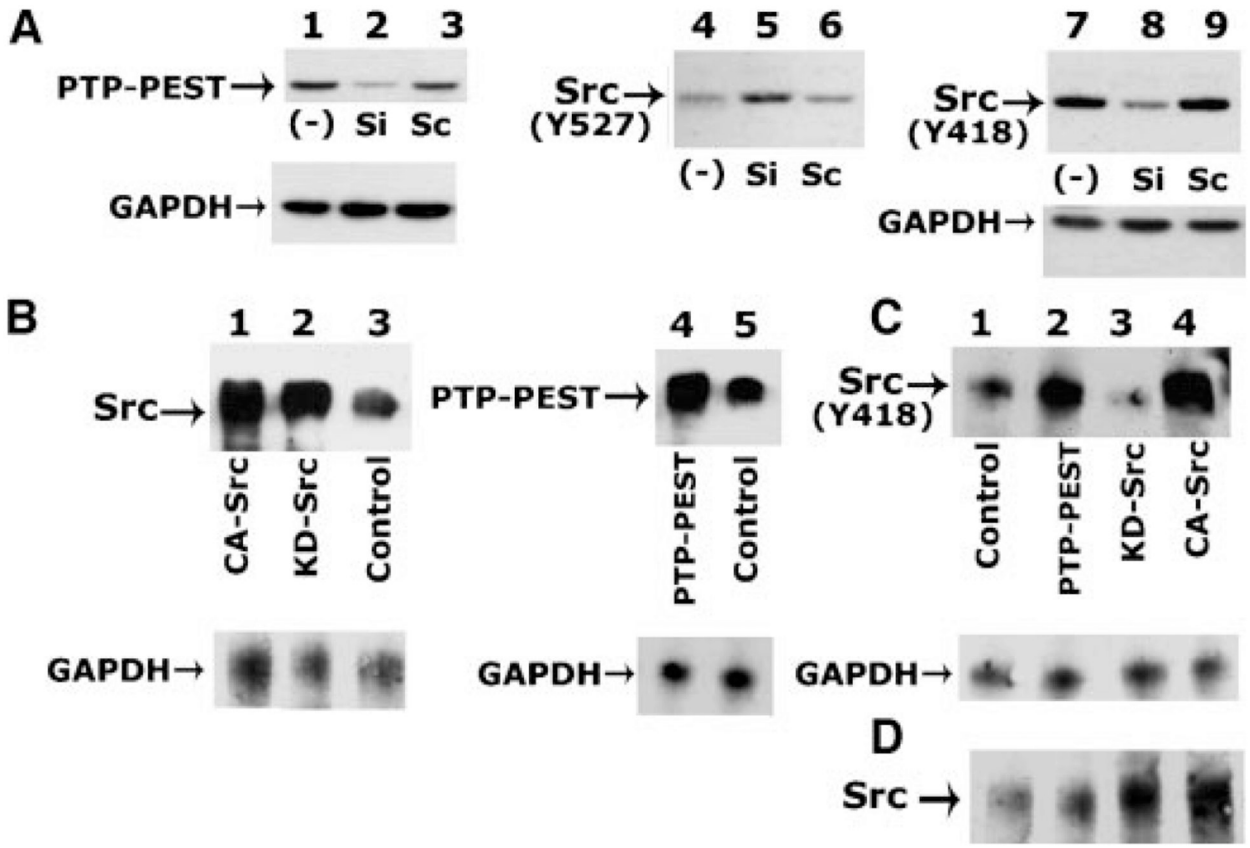

Fig. 1.

A: The effect of SiRNA to PTP–PEST on the phosphorylation of Src at Tyr418 aa residue. Immunoblotting analyses with antibodies to PTP–PEST (lanes 1–3), Src Tyr527 (lanes 4–6), and SrcY418 (lanes 7–9) are shown in cells treated as indicated in the figure. B–D: The effect of over-expression of PTP–PEST and Src (CA- and KD-Src) on the phosphorylation of Src at Tyr418 aa residue. Expression levels of Src (lanes 1–3) and PTP–PEST (lanes 4 and 5) proteins were determined by immunoblotting analyses with respective antibodies (B). Uninfected osteoclasts were used as controls (B, lanes 3 and 5). Immunoblotting analyses with antibodies to SrcTyr418 and Src are shown in parts (C) and (D). Approximately equal loading is evidenced by immunoblotting analysis with an antibody to GAPDH (A–C, bottom parts). Results shown are representative of three independent osteoclast preparation and experiments.

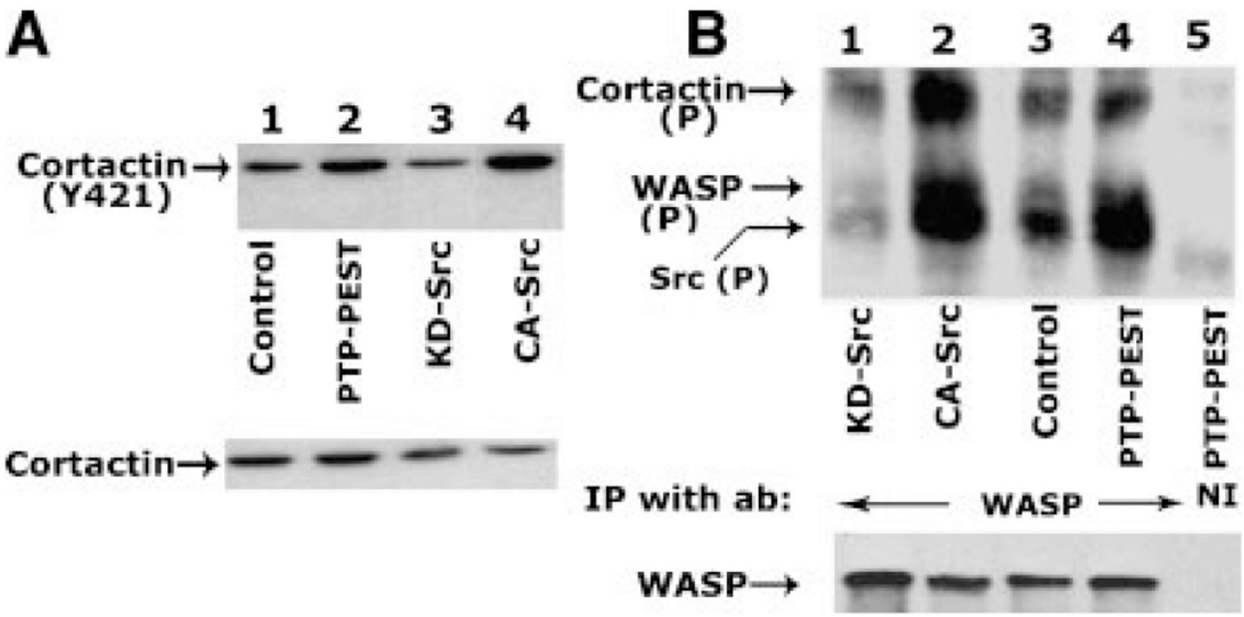

Fig. 2.

A: Analysis of the effects of over-expression of PTP–PEST and Src (CA- and KD-Src) proteins on the phosphorylation of cortactin. Immunoblotting analyses with a phosphocortactin Y421 antibody (top part) and a cortactin antibody are shown (bottom part). B: Analysis of the effects of over-expression of PTP–PEST and Src (CA- and KD-Src) proteins on the phosphorylation of WASP and WASP-associated proteins. Immunoblotting analyses with antibodies to phosphotyrosine (top part) and WASP (bottom part) are shown. The results shown are representative of three independent osteoclast preparation and experiments.

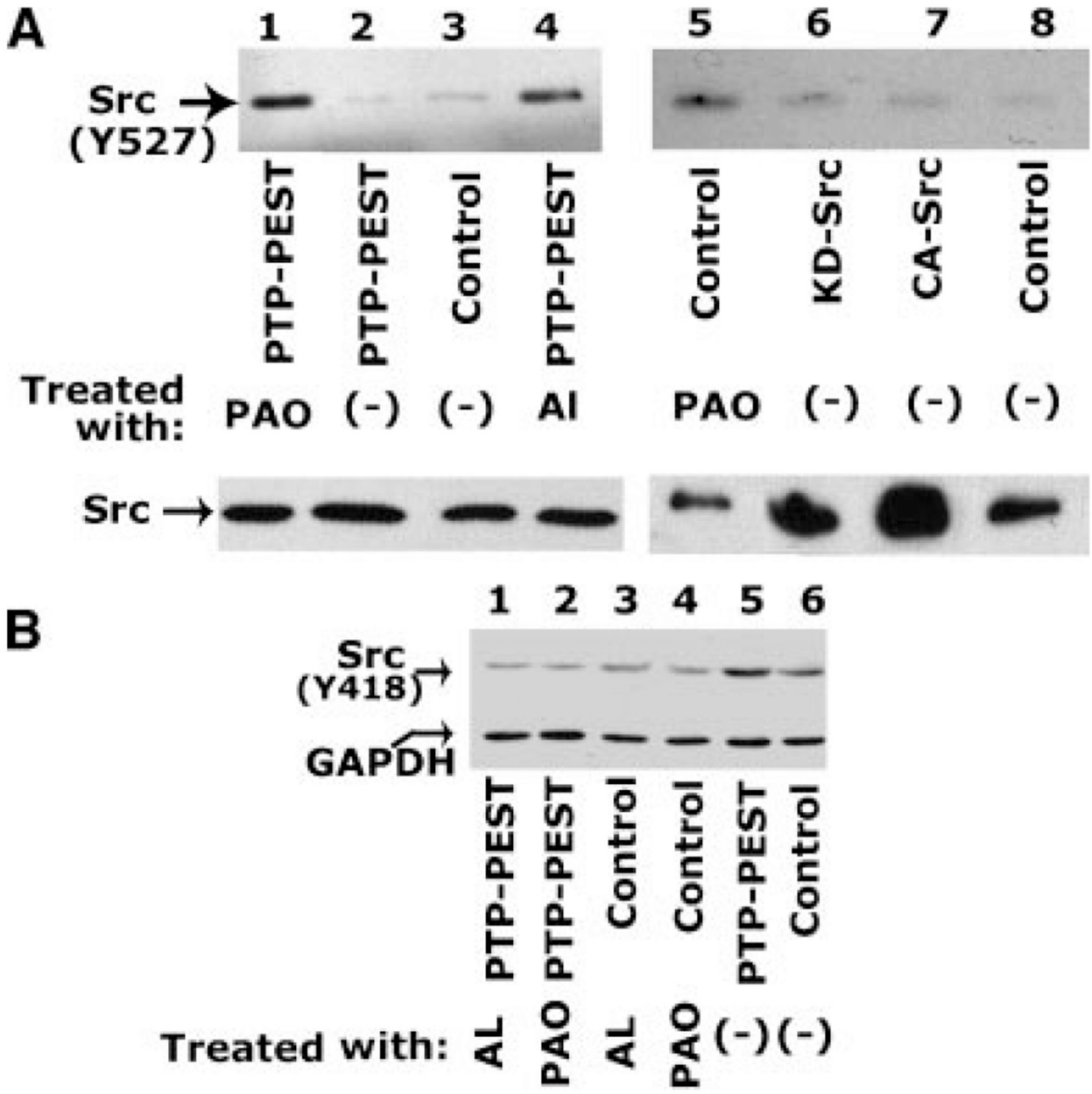

Fig. 3.

Analysis of the effects of PAO and alendronate (Al) on the tyrosine phosphorylation of Src. Osteoclasts were infected with adenovirus containing Src (KD or CA-Src) (A, lanes 6 and 7) or PTP–PEST (A and B) constructs. Control and PTP–PEST over-expressing osteoclasts were treated with PAO or alendronate as indicated below the figure (A and B). Untreated osteoclasts are represented as (−). Immunoblotting analyses with antibodies to SrcY527 (top parts) and Src (bottom parts) are shown in part (A). Immunoblotting analyses with antibodies to Src(Y418) and GAPDH are shown in part (B). Results shown are representative of three different experiments.

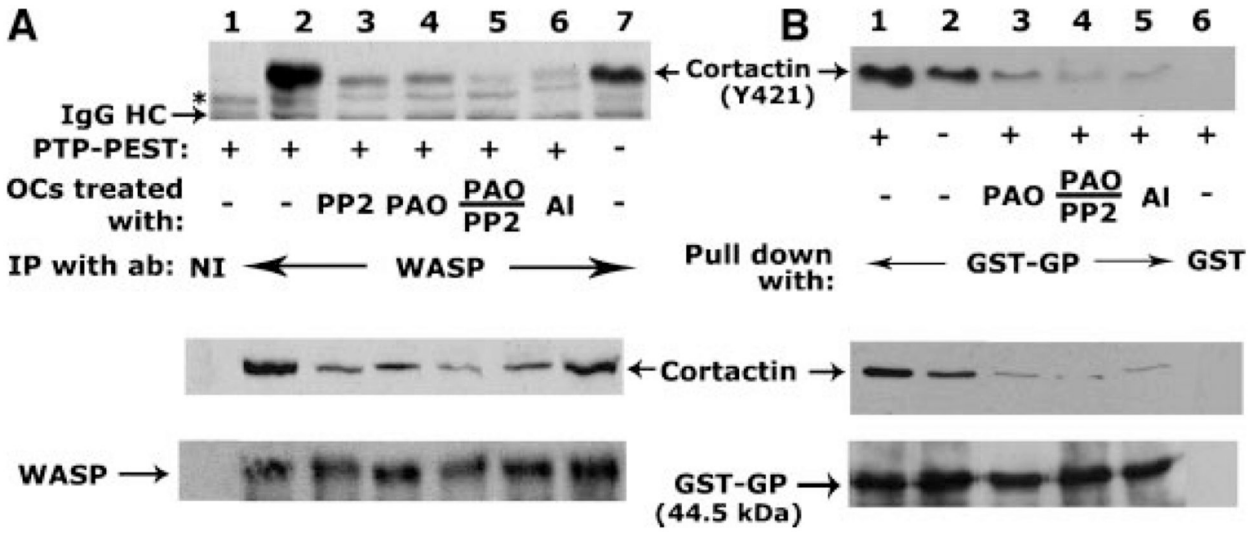

Fig. 4.

Analysis of the effects of various treatments on the phosphorylation of cortactin and its interaction with WASP. Lysates made from osteoclaststreated with various treatments as indicated below the figure are used for immunoprecipitation with a WASP antibody (A) or pulldown with GST-fused WASP-GP domain (B). Untreated osteoclasts but infected with (lane 2) and without (lane 7) adenoviral PTP–PEST constructs were used as controls. Immunoprecipitates or pulldown proteins were divided into two halves. The first part was immunoblotted (IB) with a phosphocortactin (Y421) antibody. Asterisk indicates coprecipitation of a non-specific protein, which was also observed in the NI immunoprecipitate (A, lane 1). Immunoblotting analysis of the second part with a cortactin antibody illustrates the levels of cortactin coprecipitated with WASP (A, middle part) or GST-GP (B, middle part). Stripping and reblotting of these blots with WASP or GST antibody demonstrates equal levels of WASP (A, bottom part) or GST-GP fusion protein (B, bottom part). Results shown are representative of three different experiments from three different osteoclast preparations.

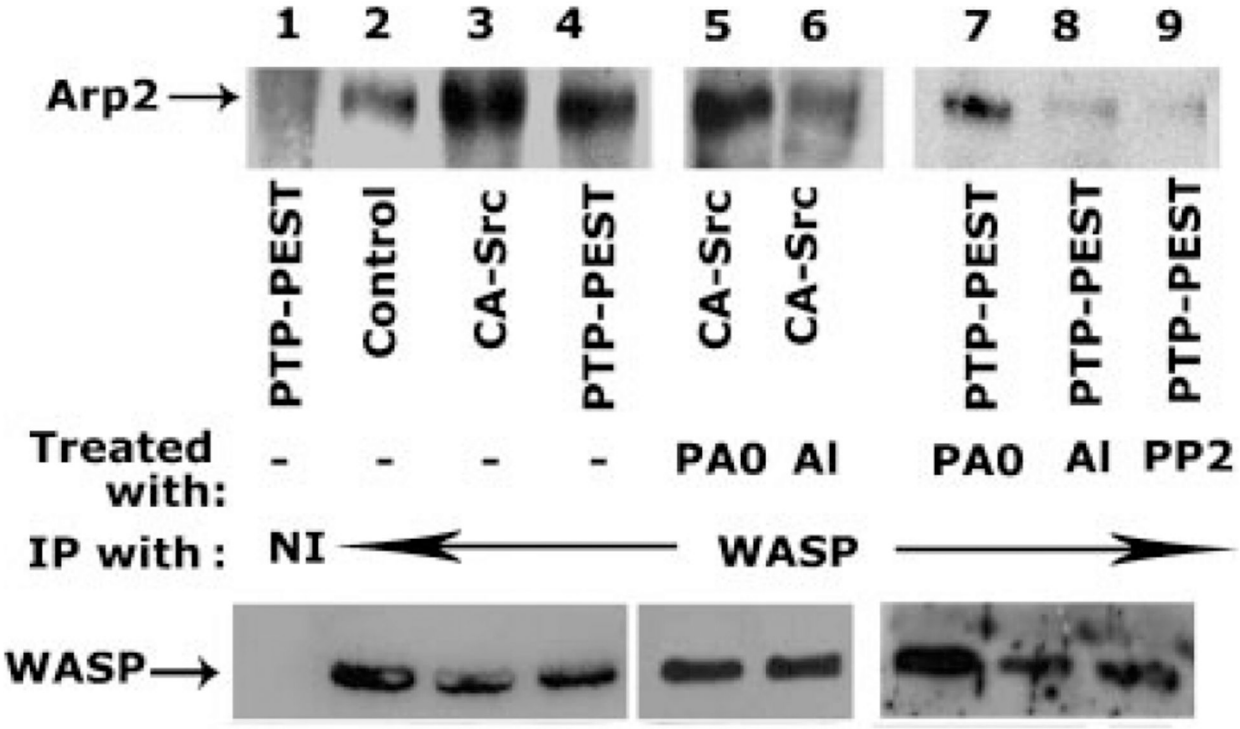

Fig. 5.

The effects of various treatments on the formation of WASP–Arp2 complex in osteoclasts. Lysate made from osteoclasts subjected to various treatments as indicated in the figure was immunoprecipitated with either a WASP antibody (lanes 2–9) or species-specific non-immune serum (NI, lane 1). Coprecipitation of Arp2 (43 kDa) protein was observed in the immunoblotting analysis (top part). This blot was stripped and reblotted with a WASP antibody to detect the levels of WASP in each immunoprecipitates (bottom part). The results shown are representative of three different experiments.

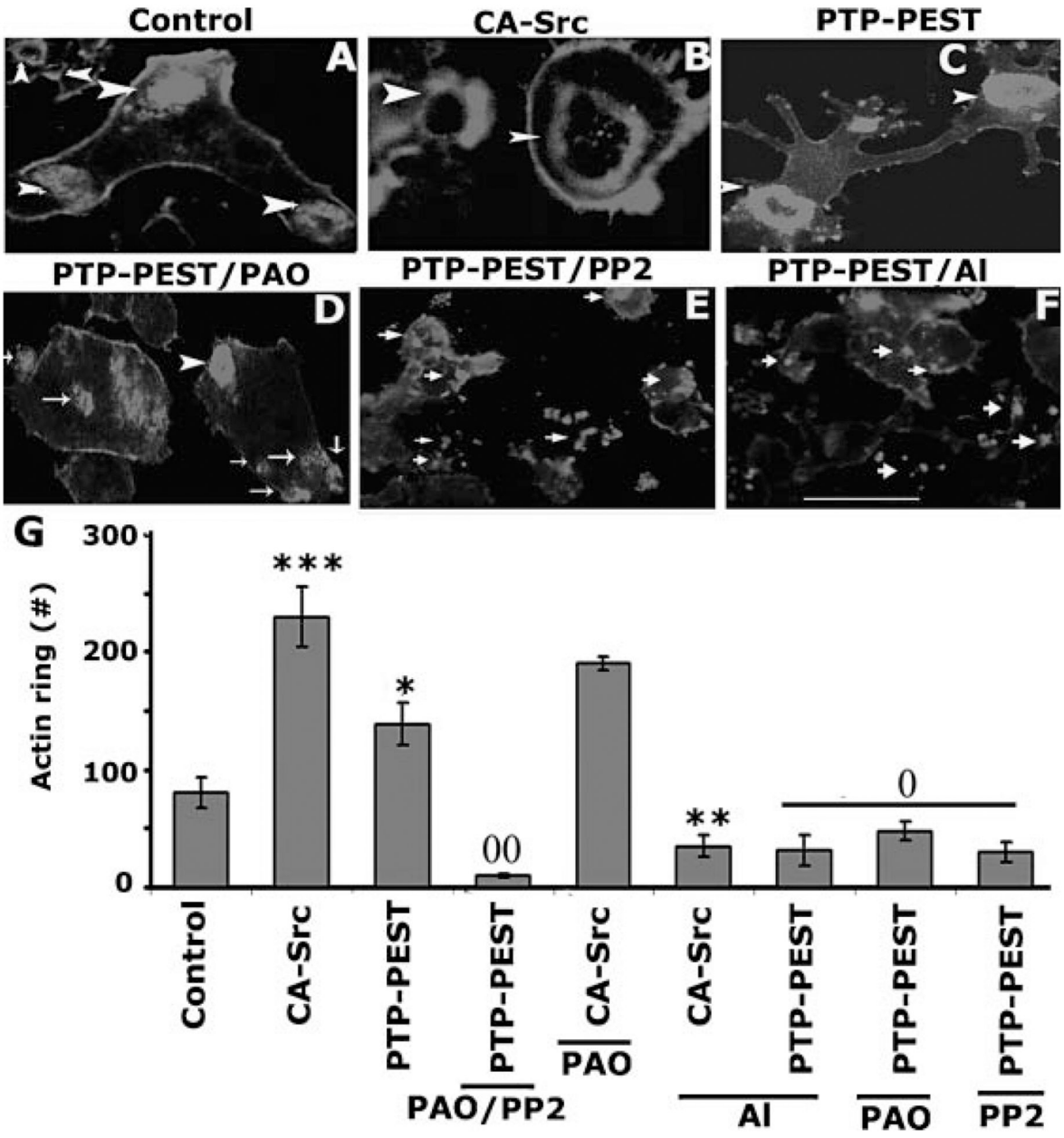

Fig. 6.

Analysis of sealing ring formation in osteoclasts subjected to various treatments. Osteoclasts were plated on dentine slices and incubated for 36–48 h at 37°C with the indicated treatments above the respective parts (A–F). Staining was performed with rhodamine phalloidin for actin. Scale bar 25 μm. The number of actin ring was determined in ~300–350 osteoclasts plated on dentine slices (G). The data are the mean W ± SE of one of three separate experiments performed with the same results. ***$P < 0.0001$, *$P < 0.01$ versus control; $^{00}P < 0.001$, $^{0}P < 0.01$ versus PTP–PEST transfectedcells; **P <0.01 versus CA-Srctransfected cells. Experiment was repeated thrice intriplicates for each treatment with osteoclasts from three separate preparations.

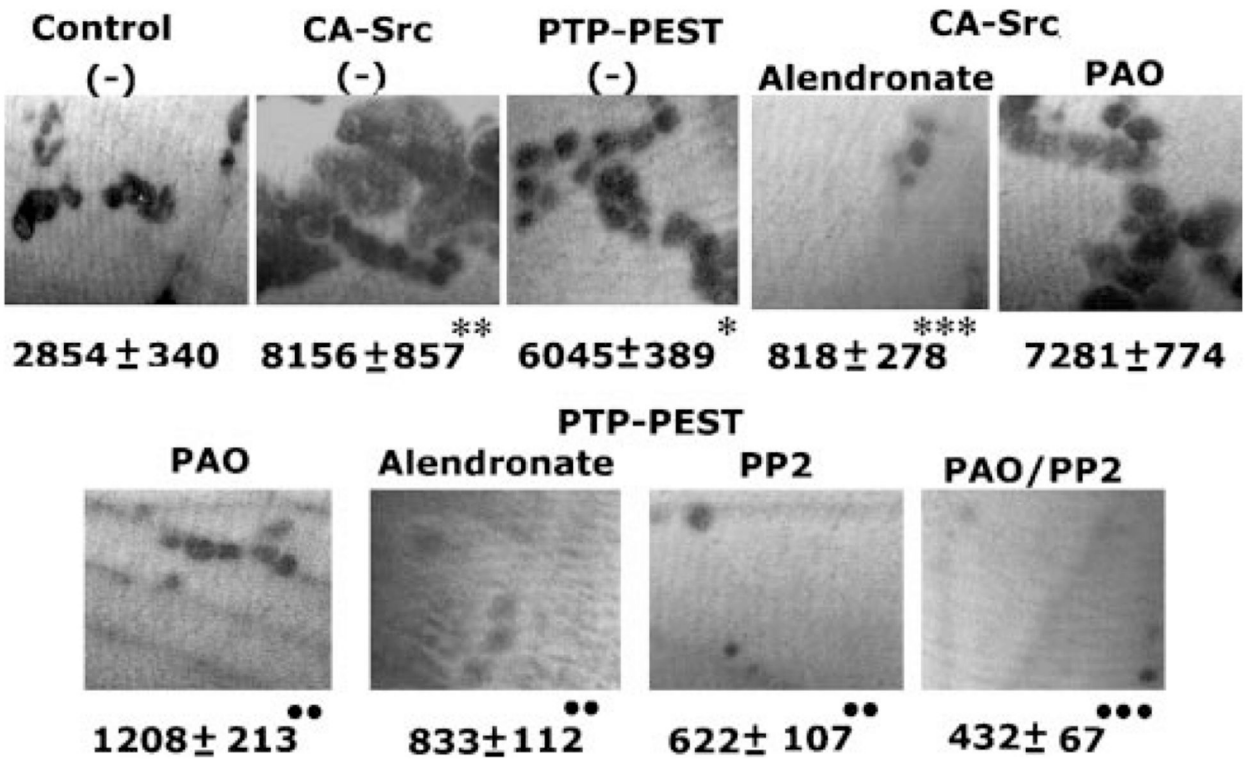

Fig. 7.

The effects of various treatments on osteoclast bone resorption in vitro. Osteoclasts were subjected to various treatments as mentioned above the respective parts for 48h. Confocalimages of resorption pits are shown.Thepitarea(μm^2)is provided at the bottom of each part.The data are mean ± SE of >100–150 resorption pits from three different dentine slices per experiment. ** $P < 0.001$, * $P < 0.01$ versus control cells; *** $p < 0.0001$ versus CA-Src transfected cells; ••• $P < 0.001$ versus PTP–PEST and CA-Src transfected cells; •• $P < 0.01$ versus PTP–PEST transfected cells. The results shown are representative of three different experiments. Experiment was repeated thrice in triplicates for each treatment with osteoclasts from three separate preparations.

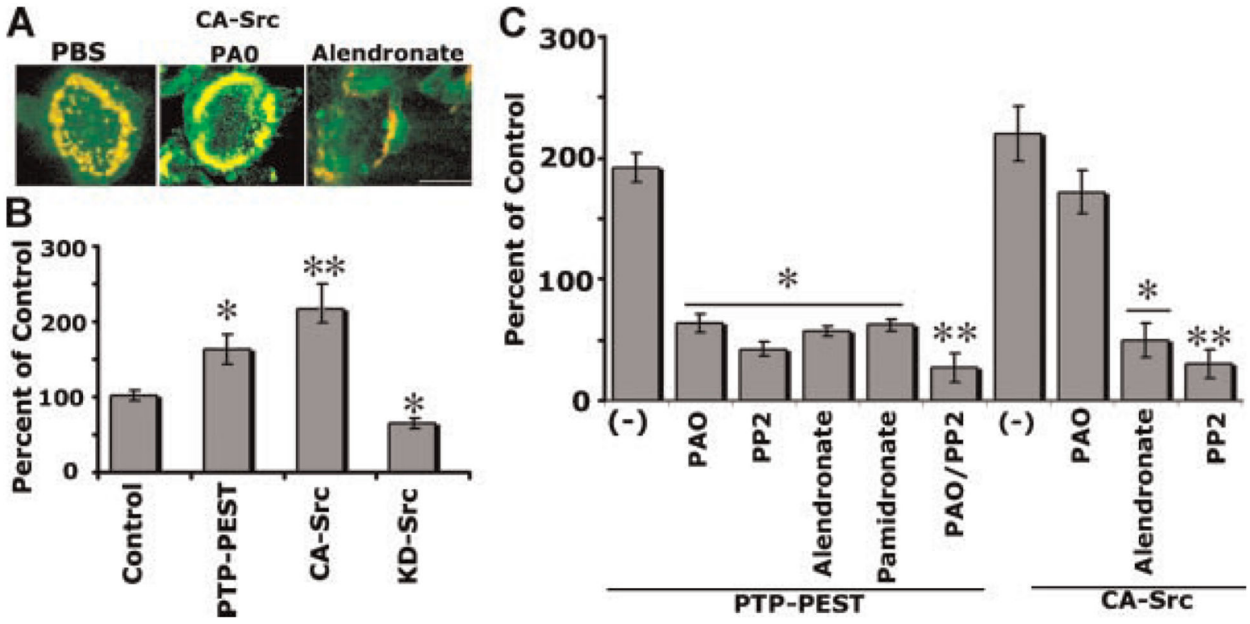

Fig. 8.

A: Analysis of the effects of various treatments on the localization of cortactinY421/actin in the sealing ring of resorbing osteoclasts. Osteoclasts expressing CA-Src protein were treated with PBS, PAO, and alendronate. Confocal microscopy images of osteoclasts stained for cortactin Y421 (green) and actin(red) are shown. Colocalization is observed in yellow color. Scalebar, 25μm. B,C:Measurement of F-actincontent. F-actin contentwas measured by rhodamine phalloidin binding in osteoclasts treated as indicated in the figure. Cells were grown in 24-well tissue culture plates, and 3–4 wells were used for each treatment.The results presented are mean ± SE for three experiments. In part (B), **P < 0.001and *P < 0.01 versus control cells. In part (C), **P < 0.001 and *P < 0.01 versus respective control (−) cells transfected with either CA-Src or PTP–PEST. Experiment was performed three times in triplicates or quadruplicates in a 24-well tissue culture plates with osteoclasts isolated from three different preparations.

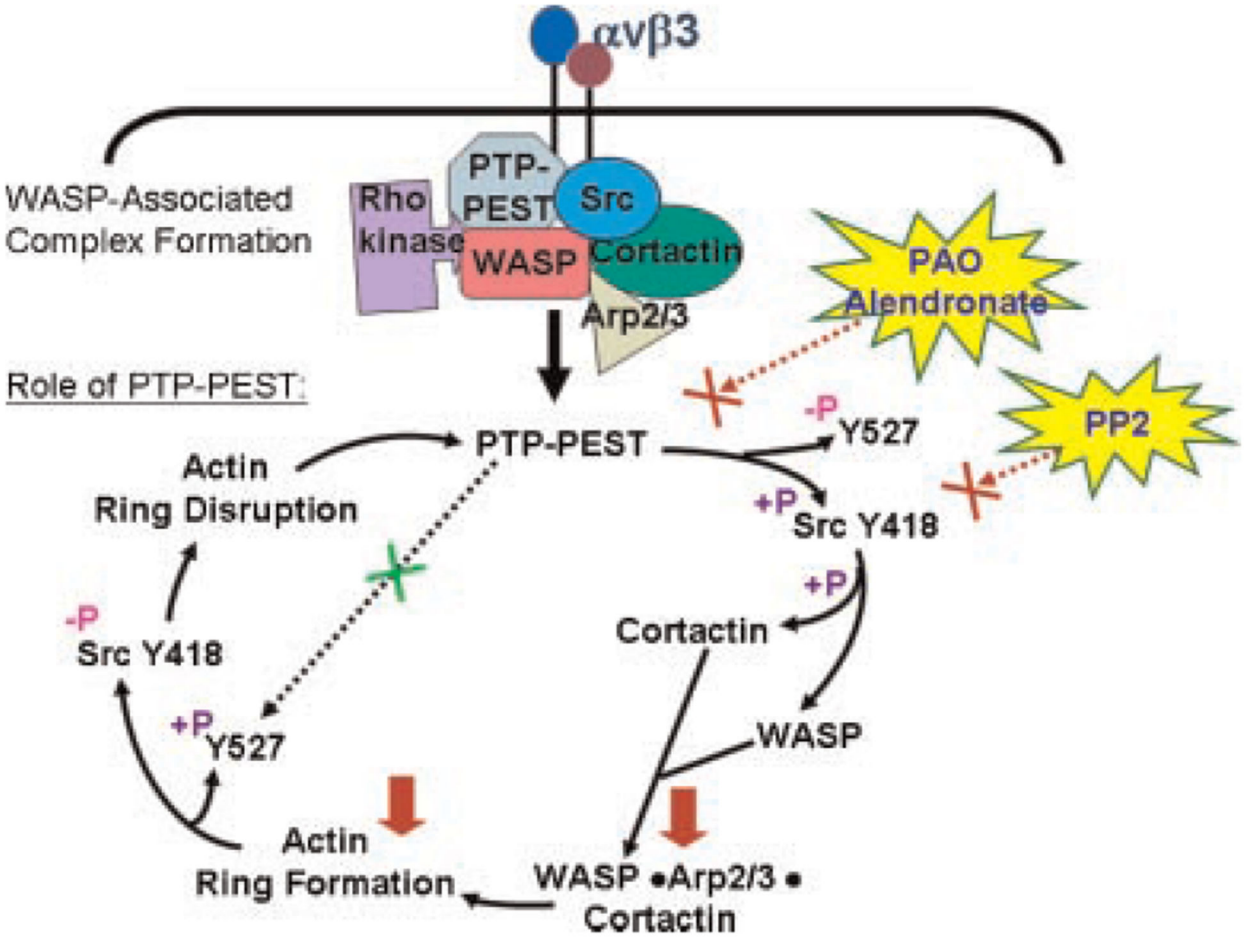

Fig. 9.

A schematic representation of the role of PTP–PEST in the activation Src kinase and actin ring formation. We have previously reported that phosphorylation of WASP and the associated signaling proteins are mediated by the cooperative function of kinase(s) and the phosphatase PTP–PEST (Chellaiah et al., 2007). Our findings of the present study on the role of PTP–PEST are as follows: (1) PTP–PEST has a role in the dephosphorylation of Src at Y527 and phosphorylation at Y418 in the catalytic site. (2) Activation of Src in osteoclasts resulted in the phosphorylation of cortactin and WASP, which resulted in the formation of WASP Arp2/3 cortactin complex. (3) This heterotrimeric complex formation is critical for cortical actin filament assembly and sealing ring formation during bone resorption. (4) Disruption of sealing ring occurs at the completion of bone resorption. This possibly occurs due to a decrease in the dephosphorylation of Src at Y527 by PTP–PEST (indicated by dotted arrows and green ‘X’) that resulted in a reduced phosphorylation state of Src atY418 and its activity. (5) Osteoclasts treated with either alendronate or PAO (indicated by dotted arrows and ‘X’ in red) decreased the phosphorylation (Y418) and activity of Src as a result of inhibition of dephosphorylation of Src at Y527 by PTP–PEST. Therefore, Src-mediated phosphorylation of cortactin and WASP as well as the formation of WASP cortactin Arp2 complex and sealing ring were reduced (indicated by inverted red

arrows). Similar effects were observed in osteoclasts treated with an Src inhibitor PP2 (indicated by dotted arrows and ‘X’ in red).